



# Ocean acidification of a coastal Antarctic marine microbial community reveals a critical threshold for CO<sub>2</sub> tolerance in phytoplankton productivity

Stacy Deppeler<sup>1</sup>, Katherina Petrou<sup>2</sup>, Kai G. Schulz<sup>3</sup>, Karen Westwood<sup>4,5</sup>, Imojen Pearce<sup>4</sup>, John McKinlay<sup>4</sup>, and Andrew Davidson<sup>4,5</sup>

<sup>1</sup>Institute for Marine and Antarctic Studies, University of Tasmania, Private Bag 129, Hobart, Tasmania 7001, Australia

<sup>2</sup>School of Life Sciences, University of Technology Sydney, 15 Broadway, Ultimo, New South Wales 2007, Australia

<sup>3</sup>Centre for Coastal Biogeochemistry, Southern Cross University, Military Rd, East Lismore, NSW 2480, Australia

<sup>4</sup>Australian Antarctic Division, Department of the Environment and Energy, 203 Channel Highway, Kingston, Tasmania 7050, Australia

<sup>5</sup>Antarctic Climate and Ecosystems Cooperative Research Centre, Private Bag 80, Hobart, Tasmania 7001, Australia

**Correspondence:** Stacy Deppeler (stacy.deppeler@utas.edu.au)

Received: 1 June 2017 – Discussion started: 29 June 2017

Revised: 10 October 2017 – Accepted: 6 November 2017 – Published: 11 January 2018

**Abstract.** High-latitude oceans are anticipated to be some of the first regions affected by ocean acidification. Despite this, the effect of ocean acidification on natural communities of Antarctic marine microbes is still not well understood. In this study we exposed an early spring, coastal marine microbial community in Prydz Bay to CO<sub>2</sub> levels ranging from ambient (343  $\mu\text{atm}$ ) to 1641  $\mu\text{atm}$  in six 650 L minicosms. Productivity assays were performed to identify whether a CO<sub>2</sub> threshold existed that led to a change in primary productivity, bacterial productivity, and the accumulation of chlorophyll *a* (Chl *a*) and particulate organic matter (POM) in the minicosms. In addition, photophysiological measurements were performed to identify possible mechanisms driving changes in the phytoplankton community. A critical threshold for tolerance to ocean acidification was identified in the phytoplankton community between 953 and 1140  $\mu\text{atm}$ . CO<sub>2</sub> levels  $\geq$  1140  $\mu\text{atm}$  negatively affected photosynthetic performance and Chl *a*-normalised primary productivity (csGPP<sub>14C</sub>), causing significant reductions in gross primary production (GPP<sub>14C</sub>), Chl *a* accumulation, nutrient uptake, and POM production. However, there was no effect of CO<sub>2</sub> on C:N ratios. Over time, the phytoplankton community acclimated to high CO<sub>2</sub> conditions, showing a down-regulation of carbon concentrating mecha-

nisms (CCMs) and likely adjusting other intracellular processes. Bacterial abundance initially increased in CO<sub>2</sub> treatments  $\geq$  953  $\mu\text{atm}$  (days 3–5), yet gross bacterial production (GBP<sub>14C</sub>) remained unchanged and cell-specific bacterial productivity (csBP<sub>14C</sub>) was reduced. Towards the end of the experiment, GBP<sub>14C</sub> and csBP<sub>14C</sub> markedly increased across all treatments regardless of CO<sub>2</sub> availability. This coincided with increased organic matter availability (POC and PON) combined with improved efficiency of carbon uptake. Changes in phytoplankton community production could have negative effects on the Antarctic food web and the biological pump, resulting in negative feedbacks on anthropogenic CO<sub>2</sub> uptake. Increases in bacterial abundance under high CO<sub>2</sub> conditions may also increase the efficiency of the microbial loop, resulting in increased organic matter remineralisation and further declines in carbon sequestration.

## 1 Introduction

The Southern Ocean (SO) is a significant sink for anthropogenic CO<sub>2</sub> (Metzl et al., 1999; Sabine et al., 2004; Frölicher et al., 2015). Approximately 30 % of anthropogenic CO<sub>2</sub> emissions have been absorbed by the world's oceans,

of which 40 % has been via the SO (Raven and Falkowski, 1999; Sabine et al., 2004; Khatiwala et al., 2009; Takahashi et al., 2009, 2012; Frölicher et al., 2015). While ameliorating CO<sub>2</sub> accumulation in the atmosphere, increasing oceanic CO<sub>2</sub> uptake alters the chemical balance of surface waters, with the average pH having already decreased by 0.1 units since pre-industrial times (Sabine et al., 2004; Raven et al., 2005). If anthropogenic emissions continue unabated, future concentrations of CO<sub>2</sub> in the atmosphere are projected to reach ~930 μatm by 2100 and peak at ~2000 μatm by 2250 (Meinshausen et al., 2011; IPCC, 2013). This will result in a further reduction of the surface ocean pH by up to 0.6 pH units, with unknown consequences for the marine microbial community (Caldeira and Wickett, 2003). High-latitude oceans have been identified as amongst the first regions to experience the negative effects of ocean acidification, causing potentially harmful reductions in the aragonite saturation state and a decline in the ocean's capacity for future CO<sub>2</sub> uptake (Sabine et al., 2004; Orr et al., 2005; McNeil and Mearns, 2008; Fabry et al., 2009; Hauck and Völker, 2015). Marine microbes play a pivotal role in the uptake and storage of CO<sub>2</sub> in the ocean through phytoplankton photosynthesis and the vertical transport of biological carbon to the deep ocean (Longhurst, 1991; Honjo, 2004). As the buffering capacity of the SO decreases over time, the biological contribution to total CO<sub>2</sub> uptake is expected to increase in importance (Hauck et al., 2015; Hauck and Völker, 2015). Thus, it is necessary to understand the effects of high CO<sub>2</sub> on the productivity of the marine microbial community if we are to predict how they may affect ocean biogeochemistry in the future.

Phytoplankton primary production provides the food source for higher trophic levels and plays a critical role in the sequestration of carbon from the atmosphere into the deep ocean (Azam et al., 1983, 1991; Longhurst, 1991; Honjo, 2004; Fenchel, 2008; Kirchman, 2008). In Antarctic waters it is restricted to a short summer season and is characterised by intense phytoplankton blooms that can reach over 200 mg Chl *a* m<sup>-2</sup> (Smith and Nelson, 1986; Nelson et al., 1987; Wright et al., 2010). Relative to elsewhere in the SO, the continental shelf around Antarctica accounts for a disproportionately high percentage of annual primary productivity (Arrigo et al., 2008a). In coastal Antarctic waters, seasonal CO<sub>2</sub> variability can be up to 450 μatm over a year (Gibson and Trull, 1999; Boyd et al., 2008; Moreau et al., 2012; Roden et al., 2013; Tortell et al., 2014). Sea ice forms a barrier to the outgassing of CO<sub>2</sub> in winter, causing supersaturation of the surface water to ~500 μatm. Intense primary productivity in summer rapidly draws down CO<sub>2</sub> to <100 μatm, making this region a significant CO<sub>2</sub> sink during summer months (Hoppema et al., 1995; Ducklow et al., 2007; Arrigo et al., 2008b).

Ocean acidification studies on individual phytoplankton species have reported differing trends in primary productivity and growth rates. Increased CO<sub>2</sub> enhanced rates of pri-

mary productivity (Wu et al., 2010; Trimborn et al., 2013) and growth (Sobrino et al., 2008; Tew et al., 2014; Baragi et al., 2015; Chen et al., 2015; King et al., 2015) in some diatom species, while others were unaffected (Chen and Durbin, 1994; Sobrino et al., 2008; Berge et al., 2010; Trimborn et al., 2013; Chen et al., 2015; Hoppe et al., 2015; King et al., 2015; Bi et al., 2017). In contrast, CO<sub>2</sub>-related declines in primary productivity and growth rate have also been observed (Barcelos e Ramos et al., 2014; Hoppe et al., 2015; King et al., 2015; Shi et al., 2017), suggesting that responses to ocean acidification are largely species specific. These differing responses among phytoplankton species may also cause changes in the composition of phytoplankton communities (Trimborn et al., 2013). It is difficult to extrapolate the response of individual species to natural communities, as monospecific studies exclude interactions among species and trophic levels. Estimates of CO<sub>2</sub> tolerance under laboratory conditions may also be influenced by experimental acclimation periods (Trimborn et al., 2014; Hennon et al., 2015; Torstensson et al., 2015; Li et al., 2017a), differences in experimental conditions (e.g. nutrients, light climate) (Hoppe et al., 2015; Hong et al., 2017; Li et al., 2017b), methods of CO<sub>2</sub> manipulation (Shi et al., 2009; Gattuso et al., 2010), and region-specific environmental adaptations (Schaum et al., 2012). Thus, investigations on natural communities are essential in order to better understand the outcome of these complex interactions.

The effects of ocean acidification on natural Antarctic phytoplankton communities is currently not well understood (Petrou et al., 2016; Deppeler and Davidson, 2017). Tolerance to CO<sub>2</sub> levels up to ~800 μatm have been reported for natural coastal communities in the West Antarctic Peninsula and Prydz Bay, East Antarctica (Young et al., 2015; Davidson et al., 2016). Although in Prydz Bay, when CO<sub>2</sub> levels exceeded 780 μatm, primary productivity declined and community composition shifted toward smaller picoeukaryotes (Davidson et al., 2016; Thomson et al., 2016; Westwood et al., 2018). In contrast, Ross Sea phytoplankton communities responded to CO<sub>2</sub> levels ≥ 750 μatm with an increase in primary productivity and abundance of large chain-forming diatoms, suggesting that as CO<sub>2</sub> increases in this region, diatoms may increase in dominance over the prymnesiophyte *Phaeocystis antarctica* (Tortell et al., 2008b; Feng et al., 2010). The paucity of information regarding the ocean acidification response of these Antarctic coastal phytoplankton communities highlights the need for further research to determine region-specific tolerances and potential tipping points in community productivity and composition in Antarctica.

Bacteria play an essential role in the microbial food web through the remineralisation of nutrients from sinking particles (Azam et al., 1991) and as a food source for heterotrophic nanoflagellates (Pearce et al., 2010). Bacterial populations respond to increases in phytoplankton primary productivity by increasing their productivity and abundance, with maximum abundance often occurring after the peak of

the phytoplankton bloom (Pearce et al., 2007). High CO<sub>2</sub> levels have been observed to have either no effect on abundance and productivity (Grossart et al., 2006; Allgaier et al., 2008; Paulino et al., 2008; Baragi et al., 2015; Wang et al., 2016) or increase growth rate and production only during the post-bloom phase of an experiment (Grossart et al., 2006; Sperling et al., 2013; Westwood et al., 2018). Thus, bacterial communities appear to be relatively tolerant to ocean acidification, with bacterial growth indirectly affected by the ocean acidification responses of the phytoplankton community (Grossart et al., 2006; Allgaier et al., 2008; Engel et al., 2013; Piontek et al., 2013; Sperling et al., 2013; Bergen et al., 2016).

Mesocosm experiments are an effective way of monitoring the community response of microbial assemblages to environmental changes. Experiments examining multiple species and trophic levels can provide responses that differ significantly from monospecific studies. Numerous mesocosm studies have now been performed to assess the effect of ocean acidification on natural marine microbial communities around the world (e.g. Kim et al., 2006; Hopkinson et al., 2010; Riebesell et al., 2013; Paul et al., 2015; Bach et al., 2016; Bunse et al., 2016). Studies in the Arctic reported increases in phytoplankton primary productivity, growth, and organic matter concentration at CO<sub>2</sub> levels  $\geq 800 \mu\text{atm}$  under nutrient-replete conditions (Bellerby et al., 2008; Egge et al., 2009; Engel et al., 2013; Schulz et al., 2013), whilst the bacterial community was unaffected (Grossart et al., 2006; Allgaier et al., 2008; Paulino et al., 2008; Baragi et al., 2015). These studies also highlight the importance of nutrient availability in the community response to elevated CO<sub>2</sub>, with substantial differences in primary and bacterial productivity, chlorophyll *a* (Chl *a*), and elemental stoichiometry observed between nutrient-replete and nutrient-limited conditions (Riebesell et al., 2013; Schulz et al., 2013; Sperling et al., 2013; Bach et al., 2016).

Previous community-level studies investigating the effects of ocean acidification on natural coastal marine microbial communities in East Antarctica reported declines in primary and bacterial productivity when CO<sub>2</sub> levels exceeded  $780 \mu\text{atm}$  (Westwood et al., 2018). To build upon the results of Westwood et al. (2018), a similar experimental design was utilised, with a natural marine microbial community from the same region exposed to CO<sub>2</sub> levels ranging from 343 to  $1641 \mu\text{atm}$  in 650 L minicosms. The methods were refined in our study to include an acclimation period to the CO<sub>2</sub> treatment under low light. Rates of primary productivity, bacterial productivity, and the accumulation of particulate organic matter (POM) were examined to ascertain whether the threshold for tolerance to CO<sub>2</sub> was similar to that reported by Westwood et al. (2018) or if acclimation affected the community response to high CO<sub>2</sub>. Photophysiological measurements were also undertaken to assess underlying mechanisms that caused shifts in phytoplankton community productivity.



**Figure 1.** Minicosm tanks filled with seawater in a temperature-controlled shipping container.

## 2 Methods

### 2.1 Minicosm set-up

Natural microbial assemblages were incubated in six 650 L polythene tanks (minicosms) housed in a temperature-controlled shipping container (Fig. 1). All minicosms were acid washed with 10 % vol : vol AR HCl, thoroughly rinsed with MilliQ water, and given a final rinse with seawater from the sampling site before use. The minicosms were filled with seawater taken amongst decomposing fast ice in Prydz Bay at Davis Station, Antarctica ( $68^{\circ}35' \text{ S}$ ,  $77^{\circ}58' \text{ E}$ ) on 19 November 2014. Water was transferred by helicopter in multiple collections using a 720 L Bambi Bucket to fill a 7000 L polypropylene holding tank. Seawater was gravity fed into the minicosm tanks through Teflon-lined hosing fitted with an in-line  $200 \mu\text{m}$  Arkal filter to exclude metazooplankton. All minicosms were filled simultaneously to ensure uniform distribution of microbes in all tanks.

The ambient water temperature at the time of sampling in Prydz Bay was  $-1.0^{\circ}\text{C}$ . Tanks were temperature controlled to an average temperature of  $0.0^{\circ}\text{C}$ , with a maximum range of  $\pm 0.5^{\circ}\text{C}$ , through the cooling of the shipping container and warming with two 300 W aquarium heaters (Fluval) that were connected to a temperature control program via Carel temperature controllers. The contents of each tank were gently mixed by a shielded high-density polyethylene auger rotating at 15 rpm, and each tank was covered with a sealed acrylic lid.

Each tank was illuminated on a 19 : 5 h light : dark cycle by two 150 W HQI-TS/NDL (Osram) metal halide lamps (transmission spectra; Deppeler et al., 2017a). The light output was filtered by a light-scattering filter and a one-quarter colour temperature (CT) blue filter (Arri) to convert the tungsten lighting to a daylight spectral distribution; attenuating wavelengths were  $< 500 \text{ nm}$  by  $\sim 20\%$  and  $> 550 \text{ nm}$  by  $\sim 40\%$  (Davidson et al., 2016).

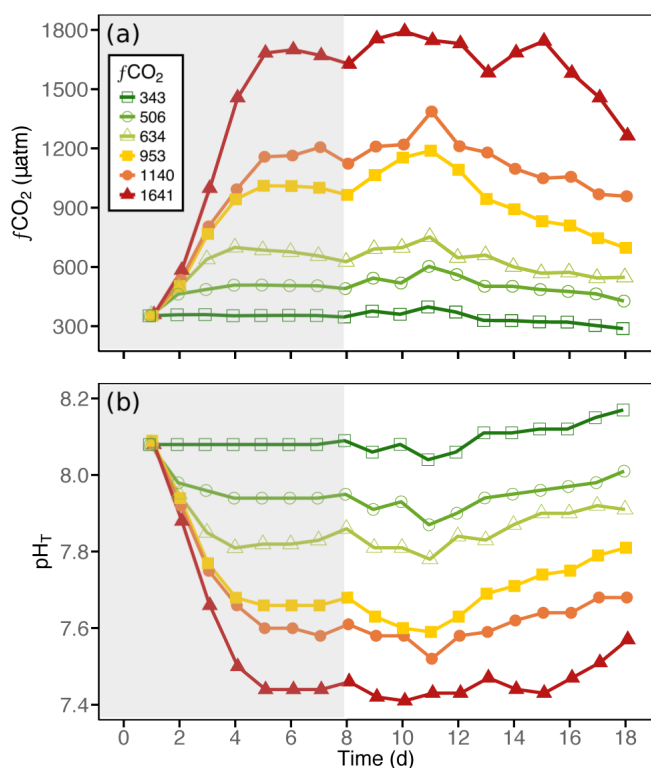


**Figure 2.** The (a)  $f\text{CO}_2$  and (b)  $\text{pH}_T$  conditions within each of the minicosm treatments over time. Grey shading indicates  $\text{CO}_2$  and light acclimation period.

Similar to Schulz et al. (2017), the fugacity of carbon dioxide ( $f\text{CO}_2$ ) in each tank was raised to the target concentration in a stepwise manner over the first 5 days of the incubation (Fig. 2, see below). During this acclimation, phytoplankton growth in the tanks was slowed by attenuating the light intensity to  $0.9 \pm 0.2 \mu\text{mol photons m}^{-2} \text{s}^{-1}$  using two 90 % neutral density (ND) filters (Arri).

At the conclusion of this  $\text{CO}_2$  acclimation period, the light intensity was increased for 24 h through the replacement of the two 90 % ND filters with one 60 % ND filter. The final light intensity was achieved on day 7 with a one-quarter CT blue and a light-scattering filter, which proved to be saturating for photosynthesis (see below).

Unless otherwise specified, samples were taken for analyses on days 1, 3, and 5 during the  $\text{CO}_2$  acclimation period and every 2 days from day 8 to 18.

## 2.2 Carbonate chemistry measurements and calculations

Samples for carbonate chemistry measurements were collected daily from each minicosm in 500 mL glass-stoppered bottles (Schott Duran) following the guidelines of Dickson et al. (2007). Subsamples for dissolved inorganic carbon (DIC; 50 mL glass-stoppered bottles) and  $\text{pH}$  on the total scale ( $\text{pH}_T$ ; 100 mL glass-stoppered bottles) measurements

were gently pressure filtered ( $0.2 \mu\text{m}$ ) with a peristaltic pump at a flow rate of  $\sim 30 \text{ mL min}^{-1}$ , similar to Bockmon and Dickson (2014).

DIC was measured by infrared absorption on an Apollo SciTech AS-C3 analyser equipped with a Li-cor LI-7000 detector using triplicate 1.5 mL samples. The instrument was calibrated (and checked for linearity) within the expected DIC concentration range with five sodium carbonate standards (Merck Suprapur) that were dried for 2 h at  $230^\circ\text{C}$  and prepared gravimetrically in MilliQ water ( $18.2 \text{ M}\Omega \text{ cm}^{-1}$ ) at  $25^\circ\text{C}$ . Furthermore, daily measurements of certified reference material batch CRM127 (Dickson, 2010) were used for improved accuracy. Volumetrically measured DIC was converted to  $\mu\text{mol kg}^{-1}$  using calculated density derived from known temperature and salinity. The typical precision among triplicate measurements was  $< 2 \mu\text{mol kg}^{-1}$ .

The  $\text{pH}_T$  was measured spectrophotometrically (GBC UV-vis 916) in a 10 cm thermostated ( $25^\circ\text{C}$ ) cuvette using the pH indicator dye m-cresol purple (Acros Organics; 62625-31-4, lot A0321770) following the approach described in Dickson et al. (2007), which included changes in sample pH due to dye addition. Contact with air was minimised by sample delivery, dye addition, and mixing via a syringe pump (Tecan; Cavro XLP 6000). Dye impurities and instrument performance were accounted for by applying a constant off-set ( $+0.003 \text{ pH units}$ ), determined by the comparison of the measured and calculated  $\text{pH}_T$  (from known DIC and total alkalinity (TA), including silicate and phosphate) of CRM127. Typical measurement precision for triplicates was 0.001 for higher and 0.003 for lower pH treatments. For further details see Schulz et al. (2017).

Carbonate chemistry speciation was calculated from measured DIC and  $\text{pH}_T$ . In a first step at salinities measured in situ (WTW197 conductivity meter), practical alkalinity (PA) was calculated at  $25^\circ\text{C}$  using the dissociation constants for carbonic acid determined by Mehrbach et al. (1973) as refitted by Lueker et al. (2000). Then, total carbonate chemistry speciation was calculated from measured DIC and calculated PA for in situ temperature conditions.

## 2.3 Carbonate chemistry manipulation

The  $f\text{CO}_2$  in the minicosms was adjusted by additions of  $0.22 \mu\text{m}$  filtered natural seawater that was saturated by bubbling with AR-grade  $\text{CO}_2$  for  $\geq 30 \text{ min}$ . In order to keep  $f\text{CO}_2$  as constant as possible throughout the experiment,  $\text{pH}$  in each minicosm was measured with a portable NBS-calibrated probe (Mettler Toledo) in the morning before sampling and in the afternoon to estimate the necessary amount of DIC to be added. The required volume of  $\text{CO}_2$ -enriched seawater was then transferred into 1000 mL infusion bags and added to the individual minicosms at a rate of about  $50 \text{ mL min}^{-1}$ . After reaching target levels, the mean  $f\text{CO}_2$  levels in the minicosms were 343, 506, 634, 953, 1140, and 1641  $\mu\text{atm}$  (Table S1 in the Supplement).

## 2.4 Light irradiance

The average light intensity in each minicosm tank was calculated by measuring light intensity in the empty tanks at three depths (top, middle, and near-bottom) and across each tank (left, middle, and right) using a Biospherical Instruments Laboratory Quantum Scalar Irradiance Meter (QSL-101). The average light irradiance received by the phytoplankton within each tank was calculated following the equation of Riley (1957) (Table 1). Incoming irradiance ( $\overline{I}_0$ ) was calculated as the average light intensity across the top of the tank. The average vertical light attenuation ( $K_d$ ) was calculated as the slope from the regression of the natural log of light intensity at all three depths, and mixed depth ( $Z_m$ ) was the depth of the minicosm tanks (1.14 m).

Changes in vertical light attenuation due to increases in Chl *a* concentration throughout the experimental period were calculated from the equation in Westwood et al. (2018);  $K_{d(\text{biomass})} = 0.0451157 \times \text{Chl } a \text{ (mg m}^{-3}\text{)}$ . Total light attenuation  $K_{d(\text{total})}$  in each tank at each sampling day was calculated by addition of  $K_d$  and  $K_{d(\text{biomass})}$ .

## 2.5 Nutrient analysis

No nutrients were added to the minicosms during the experiment. Macronutrient samples were obtained from each minicosm following the protocol of Davidson et al. (2016). Seawater was filtered through 0.45  $\mu\text{m}$  Sartorius filters into 50 mL Falcon tubes and frozen at  $-20^\circ\text{C}$  for analysis in Australia. Concentrations of ammonia, nitrate plus nitrite ( $\text{NO}_x$ ), soluble reactive phosphorus (SRP), and molybdate reactive silica (Silica) were determined using flow injection analysis by Analytical Services Tasmania following Davidson et al. (2016).

## 2.6 Elemental analysis

Samples for POM analysis, particulate organic carbon (POC), and particulate organic nitrogen (PON) were collected following the method of Pearce et al. (2007). Equipment for sample preparation was soaked in Decon 90 (Decon Laboratories) for  $> 2$  days and thoroughly rinsed in MilliQ water before use. Forceps and cutting blades were rinsed in 100 % acetone between samples. Seawater was filtered through muffled 25 mm Sartorius quartz microfibre filters until clogged. The filters were folded in half and frozen at  $-80^\circ\text{C}$  for analysis in Australia. Filters were thawed and opposite 1/8 subsamples were cut and transferred into a silver POC cup (Elemental Analysis Ltd). Inorganic carbon was removed from each sample through the addition of 20  $\mu\text{L}$  of 2N HCl to each cup and drying at  $60^\circ\text{C}$  for 36 h. When dry, each cup was folded shut, compressed into a pellet, and stored in desiccant until analysed at the Central Science Laboratory, University of Tasmania using a Thermo Finnigan EA 1112 Series Flash Elemental Analyzer.

## 2.7 Chlorophyll *a*

Seawater was collected from each minicosm and a measured volume was filtered through 13 mm Whatman GF/F filters (maximum filtration time of 20 min). Filters were folded in half, blotted dry, and immediately frozen in liquid nitrogen for analysis in Australia. Chlorophyll *a* (Chl *a*) pigments were extracted, analysed by HPLC, and quantified following the methods of Wright et al. (2010). Chl *a* was extracted from filters with 300  $\mu\text{L}$  of dimethylformamide plus 50  $\mu\text{L}$  of methanol, containing 140 ng apo-8'-carotenal (Fluka) internal standard, followed by bead beating and centrifugation to separate the extract from particulate matter. Extracts (125  $\mu\text{L}$ ) were diluted to 80 % with water and analysed on a Waters HPLC using a Waters Symmetry C8 column and a Waters 996 photodiode array detector. Chl *a* was identified by its retention time and absorption spectra compared to a mixed standard sample from known cultures (Jeffrey and Wright, 1997), which was run daily before samples. Peak integrations were performed using Waters Empower software, checked manually for corrections, and quantified using the internal standard method (Mantoura and Repeta, 1997).

## 2.8 $^{14}\text{C}$ primary productivity

Primary productivity incubations were performed following the method of Westwood et al. (2010) based on the technique of Lewis and Smith (1983). This method incubated phytoplankton for 1 h, minimising respiratory losses of photo-assimilated  $^{14}\text{C}$  so that the uptake nearly approximated gross primary productivity (e.g. Dring and Jewson, 1982; González et al., 2008; Regaudie-de Gioux et al., 2014). Samples were analysed for total organic carbon ( $\text{TO}^{14}\text{C}$ ) content, thereby including any  $^{14}\text{C}$ -labelled photosynthate leaked to the dissolved organic carbon ( $\text{DO}^{14}\text{C}$ ) pool (Regaudie-de Gioux et al., 2014).

For all samples, 5.92 MBq (0.16 mCi) of  $^{14}\text{C}$ -sodium bicarbonate ( $\text{NaH}^{14}\text{CO}_3$ ; PerkinElmer) was added to 162 mL of seawater from each minicosm, creating a working solution of 37 kBq mL $^{-1}$ . Aliquots of this working solution (7 mL) were then added to glass scintillation vials and incubated for 1 h at 21 light intensities ranging from 0–1412  $\mu\text{mol photons m}^{-2} \text{s}^{-1}$ . The temperature within each of the vials was maintained at  $-1.0 \pm 0.3^\circ\text{C}$  through water cooling of the incubation chamber. The reaction was terminated with the addition of 250  $\mu\text{L}$  of 6N HCl and the vials were shaken for 3 h at 200 rpm to remove dissolved inorganic carbon. Duplicate time zero ( $T_0$ ) samples were set up in a similar manner to determine background radiation, with 250  $\mu\text{L}$  of 6N HCl added immediately to quench the reaction without exposure to light. Duplicate 100 % samples were also performed to determine the activity of the working solution for each minicosm. For each 100 % sample, 100  $\mu\text{L}$  of working solution was added to 7 mL 0.1 M NaOH in filtered seawater to bind all  $^{14}\text{C}$ . For radioactive

counts, 10 mL of Ultima Gold LLT scintillation cocktail (PerkinElmer) was added to each scintillation vial, shaken, and decays per minute (DPM) were counted in a PerkinElmer Tri-Carb 2910TR Low Activity Liquid Scintillation Analyzer with a maximum counting time set at 3 min.

DPM counts were converted into primary productivity following the equation of Steemann Nielsen (1952) (Table 1) using measured DIC concentrations (varying between  $\sim 2075$  and  $2400 \mu\text{mol kg}^{-1}$ ) and normalised to Chl *a* using minicosm Chl *a* concentration (see above). Photosynthesis versus irradiance (PE) curves were modelled for each treatment following the equation of Platt et al. (1980) using the phytotools package in R (Silsbe and Malkin, 2015; R Core Team, 2016). Photosynthetic parameter estimates included the light-saturated photosynthetic rate ( $P_{\text{max}}$ ), maximum photosynthetic efficiency ( $\alpha$ ), photoinhibition rate ( $\beta$ ), and saturating irradiance ( $E_k$ ).

Chl *a*-specific primary productivity ( $\text{csGPP}_{14\text{C}}$ ) was calculated following the equation of Platt et al. (1980) using average minicosm light irradiance ( $\bar{I}$ ). Gross primary production rates ( $\text{GPP}_{14\text{C}}$ ) in each tank were calculated from modelled  $\text{csGPP}_{14\text{C}}$  and Chl *a* concentration (see above). Calculations and units for each parameter are presented in Table 1.

## 2.9 Gross community productivity

Community photosynthesis and respiration rates were measured using custom-made mini-chambers. The system consisted of four 5.1 mL glass vials with oxygen sensor spots (Pyro Science) attached on the inside of the vials with non-toxic silicon glue. The vials were sealed, ensuring that any oxygen bubbles were omitted, and all vials were stirred continuously using small Teflon magnetic fleas to allow homogeneous mixing of gases within the system during measurements. To improve the signal-to-noise ratio, seawater from each minicosm was concentrated above a  $0.8 \mu\text{m}$ , 47 mm diameter polycarbonate membrane filter (Poretics) with gentle vacuum filtration and resuspended in seawater from each minicosm  $\text{CO}_2$  treatment. Each chamber was filled with the cell suspension and placed in a temperature-controlled incubator ( $0.0 \pm 0.5^\circ\text{C}$ ). Light was supplied via fluorescent bulbs above each chamber and light intensity was calibrated using a  $4\pi$  sensor. Oxygen optode spots were connected to a FireSting  $\text{O}_2$  logger and data were acquired using FireSting software (Pyro Science). The optode was calibrated according to the manufacturer's protocol immediately prior to measurements using a freshly prepared sodium thiosulfate solution (10% *w/w*) and agitated filtered seawater ( $0.2 \mu\text{m}$ ) at experimental temperature for 0 and 100% air saturation values, respectively. Oxygen concentration was recorded until a linear change in rate was established for each pseudoreplicate ( $n = 4$ ).

Measurements were first recorded in the light ( $188 \mu\text{mol photons m}^{-2} \text{s}^{-1}$ ) and subsequently in the dark, with the initial steeper portion of the slope used for a

linear regression analysis to determine the post-illumination (PI) respiration rate. Gross community production ( $\text{GCP}_{\text{O}_2}$ ) was then calculated from dark PI respiration ( $\text{Resp}_{\text{O}_2}$ ) and net community production ( $\text{NCP}_{\text{O}_2}$ ) rates and normalised to Chl *a* concentration ( $\text{csGCP}_{\text{O}_2}$ , Table 1). Chl *a* content for each concentrated sample was determined by extracting pigments in 90% chilled acetone and incubating in the dark at  $4^\circ\text{C}$  for 24 h. Chl *a* concentrations were determined using a spectrophotometer (Cary 50; Varian) and calculated according to the equations of Jeffrey and Humphrey (1975), modified by Ritchie (2006).

## 2.10 Chlorophyll *a* fluorescence

The photosynthetic efficiency of the microalgal community was measured via Chl *a* fluorescence using a pulse-amplitude-modulated fluorometer (WATER-PAM; Walz). A 3 mL aliquot from each minicosm was transferred into a quartz cuvette with continuous stirring to prevent cells from settling. To establish an appropriate dark adaptation period, several replicates were measured after 5, 10, 15, 20, and 30 min of dark adaptation, with the latter having the highest maximum quantum yield of PSII ( $F_v / F_m$ ). Following dark adaptation, minimum fluorescence ( $F_0$ ) was recorded before the application of a high-intensity saturating pulse of light (saturating pulse width = 0.8 s; saturating pulse intensity  $> 3000 \mu\text{mol photons m}^{-2} \text{s}^{-1}$ ), and maximum fluorescence ( $F_m$ ) was determined. The maximum quantum yield of PSII was calculated from these two parameters (Schreiber, 2004). Following  $F_v / F_m$ , a five-step steady-state light curve (SSLC) was conducted with each light level (130, 307, 600, 973,  $1450 \mu\text{mol photons m}^{-2} \text{s}^{-1}$ ) applied for 5 min before recording the light-adapted minimum ( $F_t$ ) and maximum fluorescence ( $F_{m'}$ ) values. Each light step was spaced by a 30 s dark "recovery" period before the next light level was applied. Three pseudoreplicate measurements were conducted on each minicosm sample at  $0.1^\circ\text{C}$ . Non-photochemical quenching (NPQ) of Chl *a* fluorescence was calculated from  $F_m$  and  $F_{m'}$  measurements. Relative electron transport rates (rETR<sub>s</sub>) were calculated as the product of effective quantum yield ( $\Delta F / F_{m'}$ ) and actinic irradiance ( $I_a$ ). Calculations and units for each parameter are presented in Table 1.

## 2.11 Community carbon concentrating mechanism activity

To investigate the effects of  $\text{CO}_2$  on carbon uptake, two inhibitors for carbonic anhydrase (CA) were applied to the 343 and 1641  $\mu\text{atm}$  treatments on day 15: ethoxzolamide (EZA; Sigma), which inhibits both intracellular carbonic anhydrase (iCA) and extracellular carbonic anhydrase (eCA), and acetazolamide (AZA; Sigma), which blocks eCA only. Stock solutions of EZA (20 mM) and AZA (5 mM) were prepared in MilliQ water, and the pH was adjusted using NaOH to

Table 1. Definitions, measurements, and calculations for productivity data.

Name	Definition	Units	Measurements and calculations
<b>Primary productivity</b>			
Carbon incorporation	Total $^{14}\text{C}$ -sodium bicarbonate incorporation	$\text{mg C (mg Chl } a)^{-1} \text{ L}^{-1} \text{ h}^{-1}$	Equation from Steemann Nielsen (1952) = $\frac{(\text{DPM}_s - \text{DPM}_{t_0})}{\text{DPM}_{100\%}} \times \text{DIC} \times 1.05 / \text{time} / \text{Chl } a$
$\alpha$	Maximum photosynthetic efficiency	$\text{mg C (mg Chl } a)^{-1}$ $(\mu\text{mol photons m}^{-2} \text{ s}^{-1})^{-1} \text{ h}^{-1}$	Modelled from PE curve of 21 light intensities 0–1411 $\mu\text{mol photons m}^{-2} \text{ s}^{-1}$
$\beta$	Photoinhibition rate	$\text{mg C (mg Chl } a)^{-1}$ $(\mu\text{mol photons m}^{-2} \text{ s}^{-1})^{-1} \text{ h}^{-1}$	Modelled from PE curve of 21 light intensities 0–1411 $\mu\text{mol photons m}^{-2} \text{ s}^{-1}$
$P_{\text{max}}$	Maximum photosynthetic rate	$\text{mg C (mg Chl } a)^{-1} \text{ h}^{-1}$	Equation from Platt et al. (1980) = $P_s \times \frac{\alpha}{(\alpha + \beta)} \times \frac{\beta}{\alpha}$
$E_k$	Saturating irradiance	$\mu\text{mol photons m}^{-2} \text{ s}^{-1}$	Equation from Platt et al. (1980) = $P_{\text{max}} / \alpha$
$\bar{I}$	Average irradiance received by phytoplankton cells	$\mu\text{mol photons m}^{-2} \text{ s}^{-1}$	Equation from Riley (1957) = $\bar{I}_o (1 - e^{-(K_d \times Z_m)}) / (K_d \times Z_m)$
csGPP $^{14}\text{C}$	$^{14}\text{C}$ Chl $a$ -specific primary productivity	$\text{mg C (mg Chl } a)^{-1} \text{ h}^{-1}$	Equation from Platt et al. (1980) = $P_s \times e^{-\frac{\beta \bar{I}}{K_s}} \times e^{\frac{\beta \bar{I}}{K_s}}$
GPP $^{14}\text{C}$	$^{14}\text{C}$ gross primary production	$\mu\text{g CL}^{-1} \text{ h}^{-1}$	= csGPP $^{14}\text{C}$ $\times$ Chl $a$
csGCP $\text{O}_2$	$\text{O}_2$ Chl $a$ -specific gross community productivity	$\text{mg O}_2 \text{ (mg Chl } a)^{-1} \text{ h}^{-1}$	= (NCP $\text{O}_2$ + Res $\text{O}_2$ ) / Chl $a$
GCP $\text{O}_2$	$\text{O}_2$ gross community production	$\text{mg O}_2 \text{ L}^{-1} \text{ h}^{-1}$	= csGCP $\text{O}_2$ $\times$ Chl $a$
<b>Photophysiology</b>			
$F_v / F_m$	Maximum quantum yield of PSII	(arbitrary units)	= $(F_m - F_o) / F_m$
$\Delta F / F_m'$	Effective quantum yield of PSII	(arbitrary units)	= $(F_m' - F) / F_m'$
rETR	Relative electron transport rate	(arbitrary units)	= $\Delta F_v / F_m' \times I_a$
NPQ	Non-photochemical quenching	(arbitrary units)	= $(F_m - F_m') / F_m'$
<b>Bacterial productivity</b>			
nmol leucine $_{\text{inc}}$	Moles of exogenous $^{14}\text{C}$ -leucine incorporated	$\text{nmol L}^{-1} \text{ h}^{-1}$	Equation from Kirchman (2001) = $(\text{DPM}_s - \text{DPM}_{t_0}) / \text{time} / 2.22 \times 10^6 \times \text{SA}$ (nmol $\mu\text{Ci}^{-1}$ ) / sample vol (L)
GBP $^{14}\text{C}$	$^{14}\text{C}$ gross bacterial production	$\mu\text{g CL}^{-1} \text{ h}^{-1}$	Equation from Simon and Azam (1989) = (nmol leucine $_{\text{inc}} / 10^3$ ) $\times 131.2 / 0.073 \times 0.86 \times 2$
csBP $^{14}\text{C}$	$^{14}\text{C}$ cell-specific bacterial productivity	$\text{fg C cell}^{-1} \text{ L}^{-1} \text{ h}^{-1}$	= GBP $^{14}\text{C}$ / cells $\text{L}^{-1}$

$P_s$ : maximum photosynthetic output with no photoinhibition, from Platt et al. (1980); DPM $_s$ : sample DPM; SA: specific activity of  $^{14}\text{C}$ -leucine isotope. All other abbreviations are defined in the "Methods" section.

minimise pH changes when added to the samples. Before fluorometric measurements were made, water samples from the 343 and 1641  $\mu\text{atm}$   $\text{CO}_2$  treatments were filtered into  $\geq 10$  and  $< 10 \mu\text{m}$  fractions and aliquots were inoculated either with 50  $\mu\text{L}$  of MilliQ water adjusted with NaOH (control) or a 50  $\mu\text{M}$  final concentration of chemical inhibitor (EZA and AZA). Fluorescence measurements of size-fractionated control- and inhibitor-exposed cells were performed using the WATER-PAM. A 3 mL aliquot of sample was transferred into a quartz cuvette with stirring and left in the dark for 30 min before the maximum quantum yield of PSII ( $F_v / F_m$ ) was determined (as described above). Actinic light was then applied at 1450  $\mu\text{mol photons m}^{-2} \text{s}^{-1}$  for 5 min before the effective quantum yield of PSII ( $\Delta F / F_{m'}$ ) was recorded. Three pseudoreplicate measurements were conducted on each minicosm sample at 0.1  $^\circ\text{C}$ .

## 2.12 Bacterial abundance

Bacterial abundance was determined daily using a Becton Dickinson FACScan or FACSCalibur flow cytometer fitted with a 488 nm laser following the protocol of Thomson et al. (2016). Samples were pre-filtered through a 50  $\mu\text{m}$  mesh (Nitetex), stored at 4  $^\circ\text{C}$  in the dark, and analysed within 6 h of collection. Samples were stained for 20 min with 1 : 10000 dilution SYBR Green I (Invitrogen) (Marie et al., 2005), and PeakFlow Green 2.5  $\mu\text{m}$  beads (Invitrogen) were added to the sample as an internal fluorescence standard. Three pseudoreplicate samples were prepared from each minicosm seawater sample. Samples were run for 3 min at a low flow rate ( $\sim 12 \mu\text{L min}^{-1}$ ) and bacterial abundance was determined from side scatter (SSC) versus green (FL1) fluorescence bivariate scatter plots. The analysed volume was calibrated to the sample run time and each sample was run for precisely 3 min, resulting in an analysed volume of 0.0491 and 0.02604 mL on the FACSCalibur and FACScan, respectively. The volume analysed was then used to calculate final cell concentrations.

## 2.13 Bacterial productivity

Bacterial productivity measurements were performed following the leucine incorporation by microcentrifuge method of Kirchman (2001). Briefly, 70 nM  $^{14}\text{C}$ -leucine (PerkinElmer) was added to 1.7 mL of seawater from each minicosm in 2 mL polyethylene Eppendorf tubes and incubated for 2 h in the dark at 4  $^\circ\text{C}$ . Three pseudoreplicate samples were prepared from each minicosm seawater sample. The reaction was terminated by the addition of 90  $\mu\text{L}$  of 100 % trichloroacetic acid (TCA; Sigma) to each tube. Duplicate background controls were also performed following the same method, with 100 % TCA added immediately before incubation. After incubation, samples were spun for 15 min at 12 500 rpm and the supernatant was removed. The cell pellet was resuspended into 1.7 mL of ice-cold 5 % TCA and

spun again for 15 min at 12 500 rpm and the supernatant was removed. The cell pellet was then resuspended into 1.7 mL of ice-cold 80 % ethanol, spun for a further 15 min at 12 500 rpm, and the supernatant was removed. The cell pellet was allowed to dry completely before addition of 1 mL of Ultima Gold scintillation cocktail (PerkinElmer). The Eppendorf tubes were placed into glass scintillation vials and DPMs were counted in a PerkinElmer Tri-Carb 2910TR Low Activity Liquid Scintillation Analyzer with a maximum counting time of 3 min.

DPM counts were converted to  $^{14}\text{C}$ -leucine incorporation rates following the equation in Kirchman (2001) and used to calculate gross bacterial production ( $\text{GBP}_{^{14}\text{C}}$ ) following Simon and Azam (1989). Bacterial production was divided by total bacterial abundance to determine the cell-specific bacterial productivity within each treatment ( $\text{csBP}_{^{14}\text{C}}$ ). Calculations and units for each parameter are presented in Table 1.

## 2.14 Statistical analysis

The minicosm experimental design measured the microbial community growth in six unreplicated  $f\text{CO}_2$  treatments. Therefore, subsamples from each minicosm were within-treatment pseudoreplicates and thus only provide a measure of the variability of the within-treatment sampling and measurement procedures. We use pseudoreplicates as true replicates in order to provide an informal assessment of differences among treatments, noting that results must be treated as indicative and interpreted conservatively.

For all analyses, a linear or curved (quadratic) regression model was fitted to each  $\text{CO}_2$  treatment over time using the stats package in R (R Core Team, 2016), and an omnibus test of differences between the trends among  $\text{CO}_2$  treatments over time was assessed by ANOVA. This analysis ignored the repeated measures nature of the data set, which could not be modelled due to the low number of time points and an absence of replication at each time. For the CCM activity measurements, differences between treatments were tested by one-way ANOVA followed by a post-hoc Tukey's test to determine which treatments differed. The significance level for all tests was set at  $< 0.05$ .

## 3 Results

### 3.1 Carbonate chemistry

The  $f\text{CO}_2$  of each treatment was modified in a stepwise fashion over 5 days to allow for acclimation of the microbial community to the changed conditions. Target treatment conditions were reached in all tanks by day 5 and ranged from 343 to 1641  $\mu\text{atm}$ , equating to an average  $\text{pH}_T$  of 8.10 to 7.45 (Fig. 2, Table S1), respectively. The initial seawater was calculated to have an  $f\text{CO}_2$  of 356  $\mu\text{atm}$  and a PA of 2317  $\mu\text{mol kg}^{-1}$ , from a measured  $\text{pH}_T$  of 8.08 and DIC of 2187  $\mu\text{mol kg}^{-1}$  (Fig. S1 and Table S2 in the Supple-



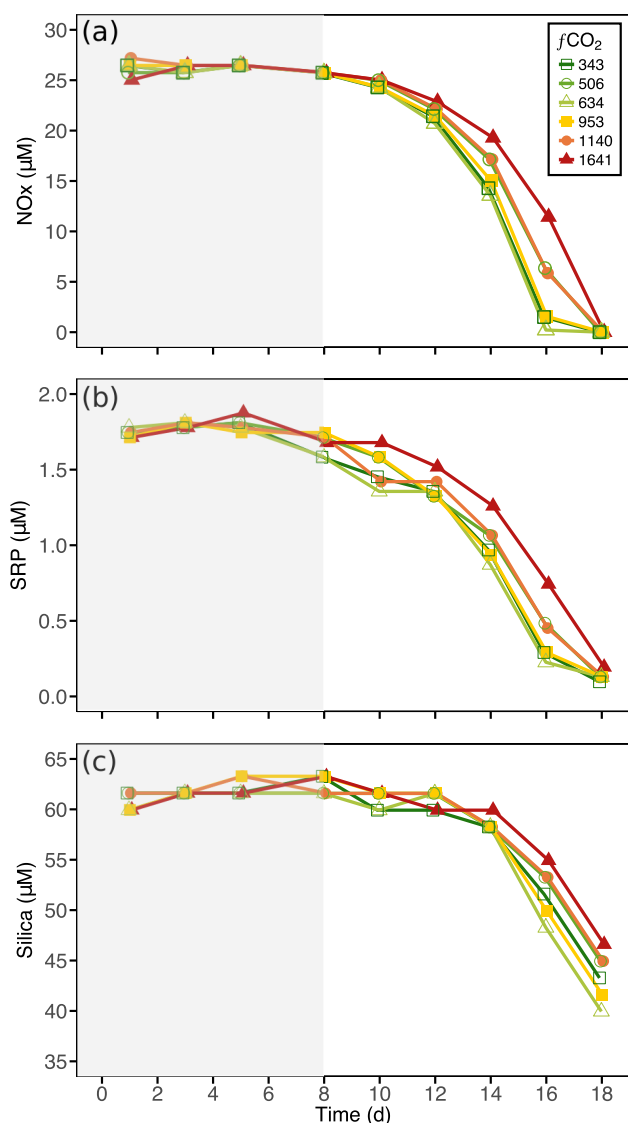


**Figure 3.** Nutrient concentration in each of the minicosm treatments over time. (a) Nitrate + nitrite ( $\text{NO}_x$ ), (b) soluble reactive phosphorus (SRP), and (c) molybdate reactive silica (silica). Grey shading indicates  $\text{CO}_2$  and light acclimation period.

ment). One minicosm was maintained close to these conditions ( $343 \mu\text{atm}$ ) throughout the experiment as a control treatment.

### 3.2 Light climate

The average light irradiance for all  $\text{CO}_2$  treatments is presented in Table S3. During the  $\text{CO}_2$  acclimation period (days 1–5) the average light irradiance was  $0.9 \pm 0.2 \mu\text{mol photons m}^{-2} \text{s}^{-1}$  and was increased to  $90.5 \pm 21.5 \mu\text{mol photons m}^{-2} \text{s}^{-1}$  by day 8. The average vertical light attenuation ( $K_d$ ) across all minicosm tanks was  $0.92 \pm 0.2$ . Increasing Chl *a* concentration over time in all

$\text{CO}_2$  treatments increased  $K_{d(\text{total})}$  from  $0.96 \pm 0.01$  on day 1 to  $3.53 \pm 0.28$  on day 18, resulting in a decline in average light irradiance within the minicosms from  $86.61 \pm 20.5$  to  $35.97 \pm 9.3 \mu\text{mol photons m}^{-2} \text{s}^{-1}$  between days 8 and 18.

### 3.3 Nutrients

Nutrient concentrations were similar across all treatments at the beginning of the experiment (Table S2 in the Supplement) and did not change during the acclimation period (days 1–5). Ammonia concentrations were initially low ( $0.95 \pm 0.18 \mu\text{M}$ ) and fell rapidly to concentrations below the limits of detection beyond day 12 in all treatments (Fig. S2 in the Supplement). No differences in drawdown between  $\text{CO}_2$  treatments were observed, and thus it was excluded from further analysis.  $\text{NO}_x$  fell from  $26.2 \pm 0.74 \mu\text{M}$  on day 8 to concentrations below detection limits on day 18 (Fig. 3a), with the slowest drawdown in the  $1641 \mu\text{atm}$  treatment. SRP concentrations were initially  $1.74 \pm 0.02 \mu\text{M}$  and all  $\text{CO}_2$  treatments followed a similar drawdown sequence to  $\text{NO}_x$ , reaching very low concentrations ( $0.13 \pm 0.03 \mu\text{M}$ ) on day 18 in all treatments (Fig. 3b). In contrast, silica was replete in all treatments throughout the experiment falling from  $60.0 \pm 0.91 \mu\text{M}$  to  $43.6 \pm 2.45 \mu\text{M}$  (Fig. 3c). The drawdown of silica was exponential from day 8 onwards and followed a similar pattern to  $\text{NO}_x$  and SRP, with the highest silica drawdown in the  $634 \mu\text{atm}$  and the least in the  $1641 \mu\text{atm}$  treatment.

### 3.4 Particulate organic matter

Particulate organic carbon (POC) and nitrogen (PON) concentrations were initially low at  $4.7 \pm 0.15$  and  $0.5 \pm 0.98 \mu\text{M}$ , respectively, and increased after day 8 in all treatments (Fig. 4a, b). The accumulation of POC and PON was effectively the reciprocal of the drawdown of nutrients (see above), being lowest in the high  $\text{CO}_2$  treatments ( $\geq 1140 \mu\text{atm}$ ) and highest in the  $343$  and  $634 \mu\text{atm}$  treatments. Rates of POC and PON accumulation were both affected by nutrient exhaustion, with declines in the  $343$  and  $634 \mu\text{atm}$  treatments between days 16 and 18. POC and PON concentrations on day 18 were highest in the  $953 \mu\text{atm}$  treatment. The ratio of POC to PON (C:N) was similar for all treatments, declining from  $8.0 \pm 0.38$  on day 8 to  $5.7 \pm 0.28$  on day 16 (Fig. 4c). The slowest initial decline in the C:N ratio occurred in the  $1641 \mu\text{atm}$  treatment, displaying a prolonged lag until day 10, after which it decreased to values similar to all other treatments. Nutrient exhaustion on day 18 coincided with an increase in the C:N ratio in all treatments, with C:N ratios  $> 10$  in the  $343$ ,  $634$ , and  $953 \mu\text{atm}$  treatments and lower C:N ratios ( $8.6$ – $6.7$ ) in the  $506$ ,  $1140$ , and  $1641 \mu\text{atm}$  treatments.

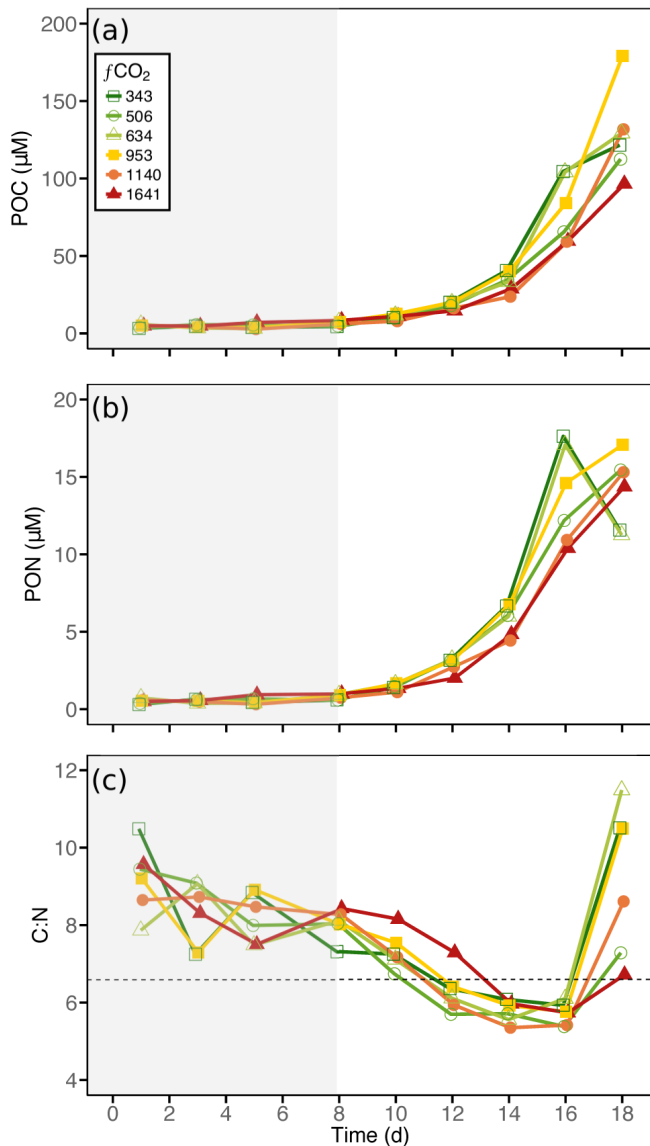


**Figure 4.** Particulate organic matter concentration and C : N ratio of each of the minicosm treatments over time. **(a)** Particulate organic carbon (POC), **(b)** particulate organic nitrogen (PON), and **(c)** carbon : nitrogen (C : N) ratio. The dashed line indicates C : N Redfield ratio of 6.6. Grey shading indicates  $\text{CO}_2$  and light acclimation period.

### 3.5 Chlorophyll *a*

Chl *a* concentrations were low at the beginning of the experiment at  $0.91 \pm 0.16 \mu\text{g L}^{-1}$  and increased in all treatments after day 8 (Fig. 5a). Chl *a* accumulation rates were similar amongst treatments  $\leq 634 \mu\text{atm}$  until day 14, with a slightly higher Chl *a* concentration in the 506 and 634  $\mu\text{atm}$  treatments on day 16 compared to the control treatment. By day 18, only the 506  $\mu\text{atm}$  treatment remained higher than the control. Chl *a* accumulation rates in the 953 and 1140  $\mu\text{atm}$  treatments were initially slow but increased after day 14, with

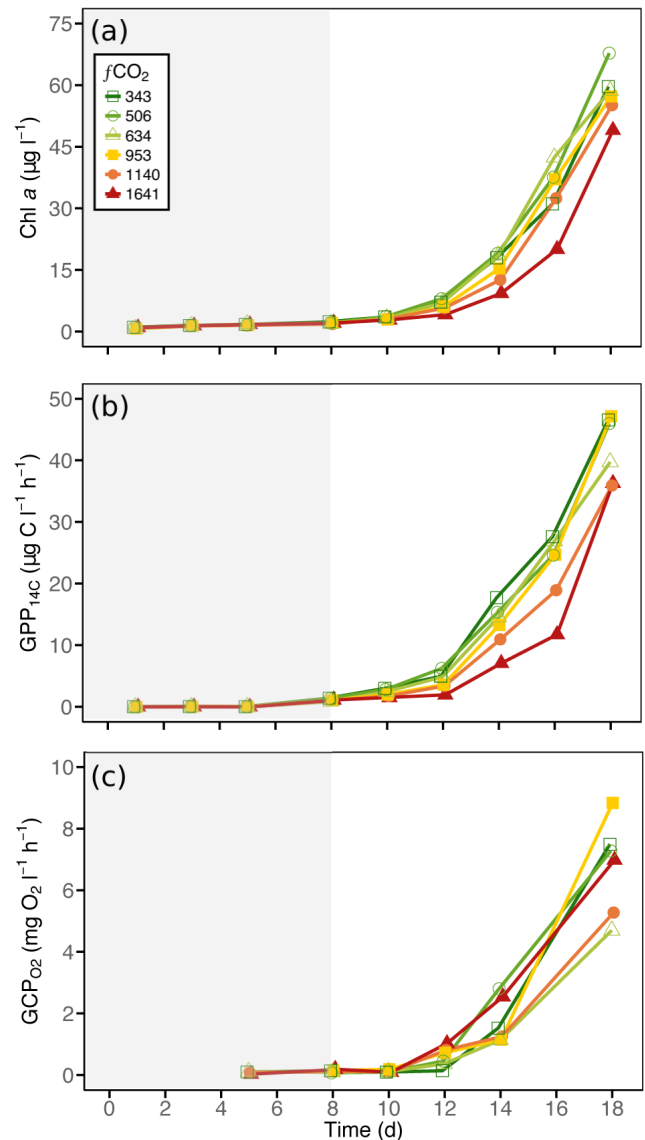


**Figure 5.** Phytoplankton biomass accumulation and community primary production in each of the minicosm treatments over time. **(a)** Chlorophyll *a* (Chl *a*) concentration, **(b)**  $^{14}\text{C}$ -derived gross primary production (GPP<sub>14C</sub>), and **(c)**  $\text{O}_2$ -derived gross community production (GCP<sub>O<sub>2</sub></sub>). Grey shading indicates  $\text{CO}_2$  and light acclimation period.

Chl *a* concentrations similar to the control on days 16–18. The highest  $\text{CO}_2$  treatment (1641  $\mu\text{atm}$ ) had the slowest rates of Chl *a* accumulation, displaying a lag in growth between days 8 and 12, after which the Chl *a* concentration increased but remained lower than the control. Rates of Chl *a* accumulation slowed between days 16 and 18 in all treatments except 1641  $\mu\text{atm}$ , coinciding with nutrient limitation. At day 18, the highest Chl *a* concentration was in the 506  $\mu\text{atm}$  exposed treatment and lowest at 1641  $\mu\text{atm}$ .

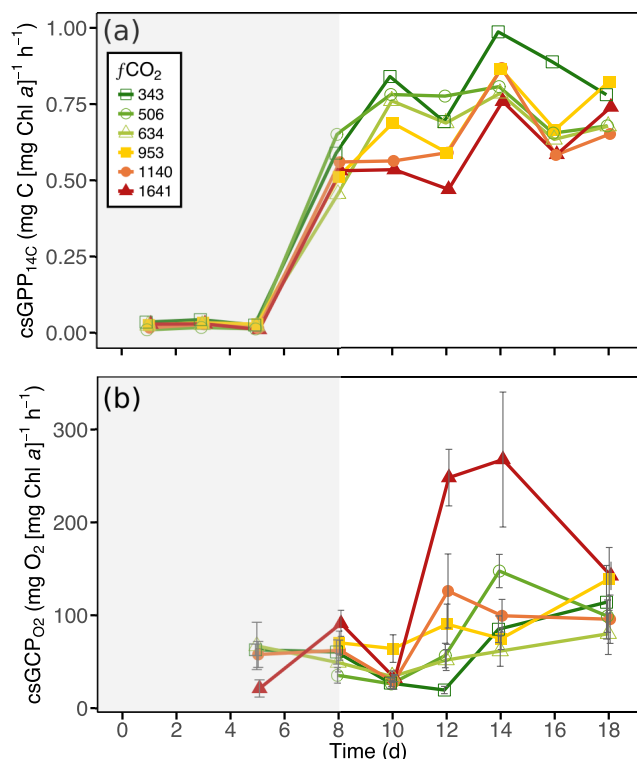


**Figure 6.** (a)  $^{14}\text{C}$ -derived Chl *a*-specific primary productivity ( $\text{csGPP}_{14\text{C}}$ ) and (b)  $\text{O}_2$ -derived Chl *a*-specific community productivity ( $\text{csGCP}_{\text{O}_2}$ ) in each of the minicosm treatments over time. Error bars display 1 standard deviation of pseudoreplicate samples. Grey shading indicates  $\text{CO}_2$  and light acclimation period.

The omnibus test among  $\text{CO}_2$  treatments of trends in Chl *a* over time indicated that the accumulation of Chl *a* in at least one treatment differed significantly from that of the control ( $F_{5,23} = 5.5$ ,  $p = 0.002$ ; Table S4). Examination of individual coefficients from the model revealed that only the highest  $\text{CO}_2$  treatment, 1641  $\mu\text{atm}$ , was significantly different from the control at the 5 % level.

### 3.6 $^{14}\text{C}$ primary productivity

During the  $\text{CO}_2$  and light acclimation phase of the experiment (days 1–8), all treatments displayed a steady decline in the maximum photosynthetic rate ( $P_{\text{max}}$ ) and the maximum photosynthetic efficiency ( $\alpha$ ) until the levels on day 8 were approximately half of those at the beginning of the experiment, suggesting cellular acclimation to the light conditions (Fig. S3a, b in the Supplement). Thereafter, relative to the control,  $P_{\text{max}}$  and  $\alpha$  were lowest in  $\text{CO}_2$  levels  $\geq 953 \mu\text{atm}$  and  $\geq 634 \mu\text{atm}$ , respectively. Rates of photoinhibition ( $\beta$ ) and saturating irradiance ( $E_k$ ) were variable and did not differ among treatments (Fig. S3c, d). The average  $E_k$  across all treatments was  $28.7 \pm 8.6 \mu\text{mol photons m}^{-2} \text{s}^{-1}$ , indicating that the light intensity in the minicosms was

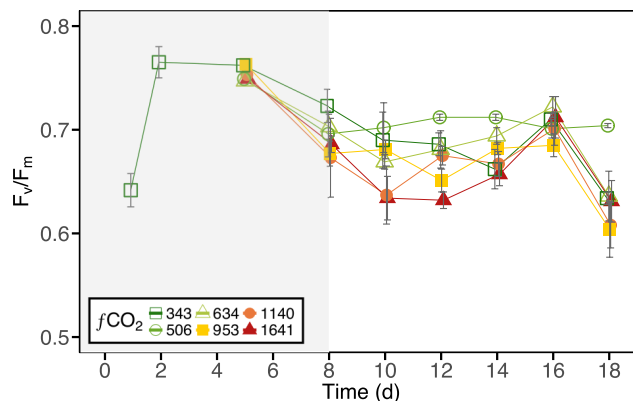


**Figure 7.** Maximum quantum yield of PSII ( $F_v / F_m$ ) in each of the minicosm treatments over time. Error bars display 1 standard deviation of pseudoreplicate samples. Grey shading indicates  $\text{CO}_2$  and light acclimation period.

saturating for photosynthesis (see above) and not inhibiting ( $\beta < 0.002 \text{ mg C (mg Chl a)}^{-1} (\mu\text{mol photons m}^{-2} \text{s}^{-1})^{-1} \text{ h}^{-1}$ ).

Chl *a*-specific primary productivity ( $\text{csGPP}_{14\text{C}}$ ) and gross primary production ( $\text{GPP}_{14\text{C}}$ ) were low during the  $\text{CO}_2$  acclimation (days 1–5) and increased with increasing light climate after day 5. Rates of  $\text{csGPP}_{14\text{C}}$  in treatments  $\geq 634 \mu\text{atm}$   $\text{CO}_2$  were consistently lower than the control between days 8 and 16, with the lowest rates in the highest  $\text{CO}_2$  treatment (1641  $\mu\text{atm}$ ; Fig. 6a). Rates of  $\text{GPP}_{14\text{C}}$  in treatments  $\leq 953$  were similar between days 8 and 16, with the 343 (control), 506, and 953  $\mu\text{atm}$  treatments increasing to  $46.7 \pm 0.34 \mu\text{g CL}^{-1} \text{ h}^{-1}$  by day 18 (Fig. 5b). Compared to these treatments,  $\text{GPP}_{14\text{C}}$  in the 634  $\mu\text{atm}$  treatment was lower on day 18, only reaching  $39.7 \mu\text{g CL}^{-1} \text{ h}^{-1}$ , possibly due to the concurrent limitation of  $\text{NO}_x$  in this treatment on day 16 (see above).

The omnibus test among tanks of the trends in  $\text{CO}_2$  treatments over time indicated that  $\text{GPP}_{14\text{C}}$  in at least one treatment differed significantly from the control ( $F_{5,23} = 4.9$ ,  $p = 0.003$ ; Table S5 in the Supplement). Examination of the significance of individual curve terms revealed that this manifested as differences between the 1140 and 1641  $\mu\text{atm}$  treatments and the control group at the 5 % level. No other curves were different from the control. In particular,  $\text{GPP}_{14\text{C}}$  in the 1641  $\mu\text{atm}$  treatment was much lower until day 12, after which it increased steadily until day 16. Between days 16 and 18, a substantial increase in  $\text{GPP}_{14\text{C}}$  was observed in this treatment, subsequently resulting in a rate on day 18 that was similar to the 1140  $\mu\text{atm}$  treatment ( $36.3 \pm 0.08 \mu\text{g CL}^{-1} \text{ h}^{-1}$ ) although these treatments never reached rates of  $\text{GPP}_{14\text{C}}$  as high as the control.

### 3.7 Gross community productivity

The productivity of the phytoplankton community increased over time in all  $\text{CO}_2$  treatments; however, there were

clear differences in the timing and magnitude of this increase between treatments (Fig. 6b). A CO<sub>2</sub> effect was evident on day 12 when Chl *a*-normalised gross O<sub>2</sub> productivity rates (csGCP<sub>O<sub>2</sub></sub>) increased with increasing CO<sub>2</sub> level, ranging from 19.5–248 mg O<sub>2</sub> (mg Chl *a*)<sup>-1</sup> h<sup>-1</sup>. After day 12, the communities in CO<sub>2</sub> treatments ≤ 634 μatm continued to increase their rates of csGCP<sub>O<sub>2</sub></sub> until day 18 (97.7 ± 17.0 mg O<sub>2</sub> (mg Chl *a*)<sup>-1</sup> h<sup>-1</sup>). The 953 and 1140 μatm CO<sub>2</sub> treatments peaked on day 12 (90.4 and 126 mg O<sub>2</sub> (mg Chl *a*)<sup>-1</sup> h<sup>-1</sup>, respectively) and then declined on day 14 to rates similar to the control treatment. In contrast, the 1641 μatm treatment maintained high rates of csGCP<sub>O<sub>2</sub></sub> from days 12–14 (258 ± 13.8 mg O<sub>2</sub> (mg Chl *a*)<sup>-1</sup> h<sup>-1</sup>), coinciding with the recovery of photosynthetic health ( $F_v / F_m$ ; see below) and the initiation of growth in this treatment (see above). After this time, rates of csGCP<sub>O<sub>2</sub></sub> declined in this treatment to rates similar to the control. Despite these differences in csGCP<sub>O<sub>2</sub></sub>, there was no significant difference in the gross community production (GCP<sub>O<sub>2</sub></sub>) among CO<sub>2</sub> treatments (Fig. 5c).

### 3.8 Community photosynthetic efficiency

The community maximum quantum yield of PSII ( $F_v / F_m$ ) showed a dynamic response over the duration of the experiment (Fig. 7). Values initially increased during the low-light CO<sub>2</sub> adjustment period but declined by day 8 when irradiance levels had increased. Between days 8 and 14, differences were evident in the photosynthetic health of the phytoplankton community across the CO<sub>2</sub> treatments, although by day 16 these differences had disappeared. Steady-state light curves revealed that the community photosynthetic response did not change with increasing CO<sub>2</sub>. The effective quantum yield of PSII ( $\Delta F / F_m'$ ) and NPQ showed no variability with CO<sub>2</sub> treatment (Figs. S5 and S6 in the Supplement). There was, however, a notable decline in overall NPQ in all tanks with time, indicating an adjustment to the higher light conditions. Relative electron transport rates (rETR) showed differentiation with respect to CO<sub>2</sub> at high light (1450 μmol photons m<sup>-2</sup> s<sup>-1</sup>) on days 10–12. However, as seen with the  $F_v / F_m$  response, this difference was diminished by day 18 (Fig. S7 in the Supplement).

### 3.9 Community CCM activity

There was a significant decline in the effective quantum yield of PSII ( $\Delta F / F_m'$ ) with the addition of the iCA and eCA inhibitor EZA to both the large (≥ 10 μm,  $p = 0.02$ ) and small (< 10 μm,  $p < 0.001$ ) size fractions of the phytoplankton community exposed to the control (343 μatm) CO<sub>2</sub> treatment (Fig. 8). The addition of EZA to cells under high CO<sub>2</sub> (1641 μatm) had no effect on  $\Delta F / F_m'$  for either size fraction. However, in the case of the small cells under high CO<sub>2</sub> (Fig. 8b),  $\Delta F / F_m'$  was the same as that measured in the control CO<sub>2</sub> in the presence of EZA. The addition of AZA,

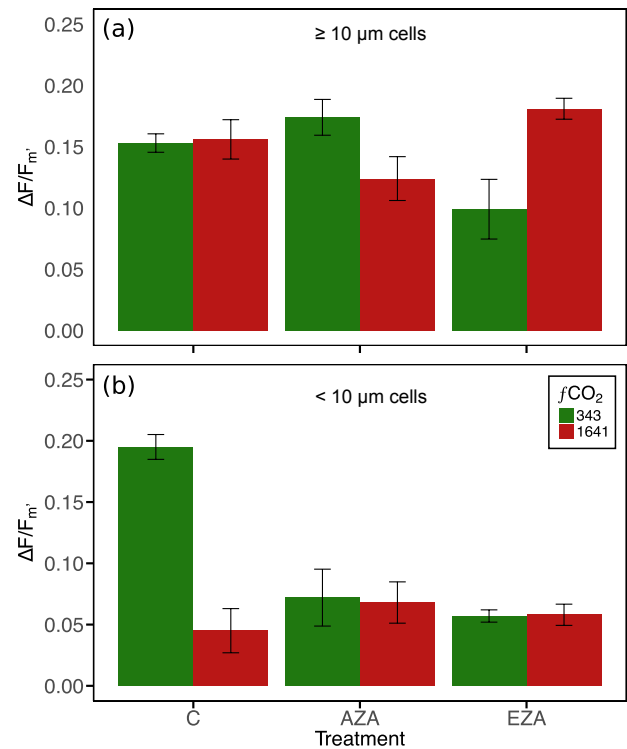


**Figure 8.** Effective quantum yield of PSII ( $\Delta F / F_m'$ ) of (a) large (≥ 10 μm) and (b) small (< 10 μm) phytoplankton in the control (343 μatm) and high (1641 μatm) CO<sub>2</sub> treatments treated with carbonic anhydrase (CA) inhibitors. A decline in  $\Delta F / F_m'$  with the application of inhibitor indicates CCM activity. C denotes the control treatment, which received no CA inhibitor; AZA is the acetazolamide treatment, which blocks extracellular carbonic anhydrase; EZA is the ethoxzolamide treatment, which blocks intracellular and extracellular carbonic anhydrase. Error bars display 1 standard deviation of pseudoreplicate samples.

which inhibits eCA only, had no effect for either CO<sub>2</sub> treatment in the large-celled community. In contrast, there was a significant decline in  $\Delta F / F_m'$  in the smaller fraction in the control CO<sub>2</sub> treatment ( $p < 0.001$ ), but no effect of AZA addition under high CO<sub>2</sub>. Again, the high CO<sub>2</sub> cells exhibited the same  $\Delta F / F_m'$  as those measured under the control CO<sub>2</sub> in the presence of AZA.

### 3.10 Bacterial abundance

During the 8-day acclimation period, bacterial abundance in treatments ≥ 634 μatm increased with increasing CO<sub>2</sub>, reaching 26.0–32.4 × 10<sup>7</sup> cells L<sup>-1</sup> and remaining high until day 13 (Fig. 9a). Between days 7 and 13, bacterial abundances in CO<sub>2</sub> treatments ≥ 953 were higher than the control. In contrast, abundance remained constant in treatments ≤ 506 μatm (20.6 ± 1.4 × 10<sup>7</sup> cells L<sup>-1</sup>) until day 11. Cell numbers rapidly declined in all treatments after day 12, finally stabilising at 0.5 ± 0.2 × 10<sup>7</sup> cells L<sup>-1</sup>. An omnibus test

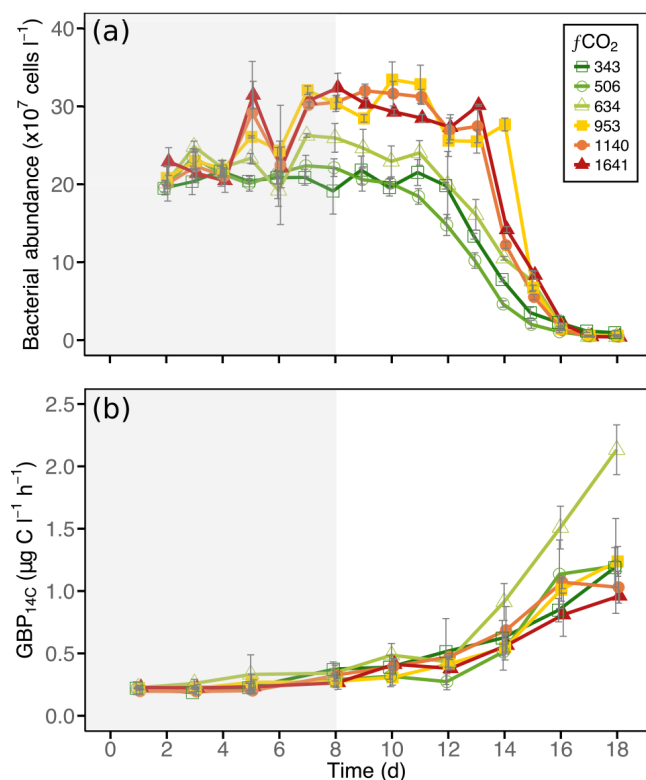


**Figure 9.** Bacterial abundance and community production in each of the minicosm treatments over time. **(a)** Bacterial cell abundance and **(b)** <sup>14</sup>C-derived gross bacterial production (GBP<sub>14C</sub>). Error bars display 1 standard deviation of pseudoreplicate samples. Grey shading indicates CO<sub>2</sub> and light acclimation period.

among CO<sub>2</sub> treatments of the trends in bacterial abundance over time showed that changes in abundance in at least one treatment differed significantly from the control ( $F_{5,185} = 9.8$ ,  $p < 0.001$ ; Table S6 in the Supplement). Examination of individual coefficients from the model revealed that CO<sub>2</sub> treatments  $\geq 953$  µatm were significantly different from the control at the 5% level.

### 3.11 Bacterial productivity

Gross bacterial production (GBP<sub>14C</sub>) was low in all CO<sub>2</sub> treatments ( $0.2 \pm 0.03$  µg CL<sup>-1</sup> h<sup>-1</sup>) and changed little during the first 5 days of incubation (Fig. 9b). Thereafter it increased, coinciding with exponential growth in the phytoplankton community. The most rapid increase in GBP<sub>14C</sub> was observed in the 634 µatm treatment, resulting in a rate twice that of all other treatments by day 18 ( $2.1$  µg CL<sup>-1</sup> h<sup>-1</sup>). No difference was observed among other treatments, all of which increased to an average rate of  $1.1 \pm 0.1$  µg CL<sup>-1</sup> h<sup>-1</sup> by day 18. Cell-specific bacterial productivity (csBP<sub>14C</sub>) was low in all treatments ( $1.2 \pm 0.5$  fg CL<sup>-1</sup> h<sup>-1</sup>) until day 14, with slower rates in treatments  $\geq 953$  µatm, likely due to high cell abundances observed in these treatments (Fig. S8

in the Supplement). It then increased from day 14, coinciding with a decline in bacterial abundance. Rates of csBP<sub>14C</sub> did not differ among treatments until day 18, when the rate in the 634 µatm treatment was higher than all other treatments ( $0.5$  pg C cell<sup>-1</sup> L<sup>-1</sup> h<sup>-1</sup>).

## 4 Discussion

Our study of a natural Antarctic phytoplankton community identified a critical threshold for tolerance of CO<sub>2</sub> between 953 and 1140 µatm, above which photosynthetic health was negatively affected and rates of carbon fixation and Chl *a* accumulation declined. Low rates of primary productivity also led to declines in nutrient uptake rates and POM production, although there was no effect of CO<sub>2</sub> on C:N ratios, indicating that ocean acidification effects on the phytoplankton community did not modify POM stoichiometry. Assessing the temporal trends of Chl *a*, GPP<sub>14C</sub>, and PON against CO<sub>2</sub> treatment revealed that the downturn in these parameters occurred between 634 and 953 µatm fCO<sub>2</sub> and could be discerned following  $\geq 12$  days incubation (Fig. 10). On the final day of the experiment (day 18), this CO<sub>2</sub> threshold was less clear and likely confounded by the effects of nutrient limitation (Westwood et al., 2018). In contrast, bacterial productivity was unaffected by increased CO<sub>2</sub>. Instead, production coincided with increased organic matter supply from phytoplankton primary productivity. In the following sections these effects will be investigated further, with suggestions for possible mechanisms that may be driving the responses observed.

### 4.1 Ocean acidification effects on phytoplankton productivity

The results of this study suggest that exposing phytoplankton to high CO<sub>2</sub> levels can decouple the two stages of photosynthesis (see also the discussion below). At CO<sub>2</sub> levels  $\geq 1140$  µatm, Chl *a*-specific oxygen production (csGCP<sub>O<sub>2</sub></sub>) increased strongly yet displayed the lowest rates of Chl *a*-specific carbon fixation (csGPP<sub>14C</sub>; Fig. 6). This mismatch in oxygen production and carbon fixation is likely due to the two-stage process in the photosynthetic fixation of carbon (reviewed in Behrenfeld et al., 2004). In the first stage, light-dependent reactions occur within the chloroplast, converting light energy (photons) into the cellular energy products, adenosine triphosphate (ATP), and nicotinamide adenine dinucleotide phosphate (NADPH), producing O<sub>2</sub> as a by-product. This cellular energy is then utilised in a second, light-independent pathway, which uses the carbon-fixing enzyme RuBisCO to convert CO<sub>2</sub> into sugars through the Calvin cycle. However, under certain circumstances the relative pool of energy may also be consumed in alternative pathways, such as respiration and photoprotection (Behrenfeld et al., 2004; Gao and Campbell, 2014). Increases in en-

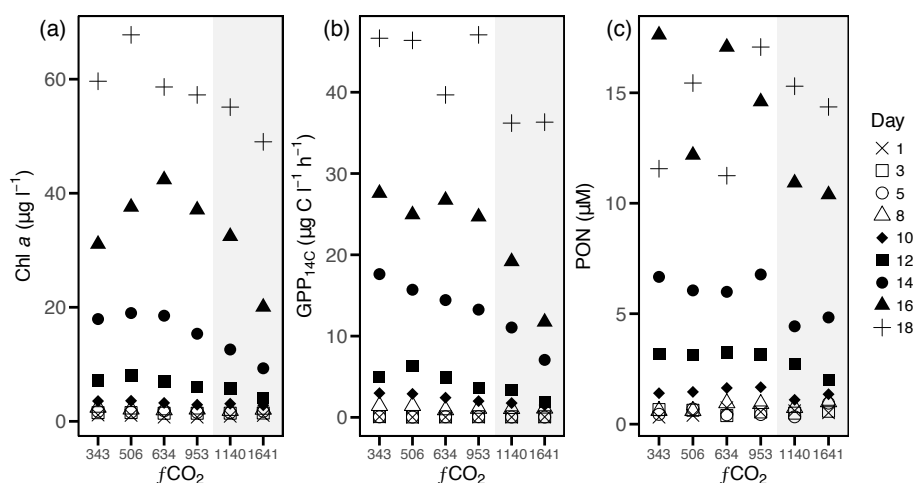


**Figure 10.** Temporal trends of (a) Chl *a*, (b)  $^{14}\text{C}$ -derived gross primary production ( $\text{GPP}_{14\text{C}}$ ), and (c) particulate organic nitrogen (PON) against  $\text{CO}_2$  treatment. Grey shading indicates  $\text{CO}_2$  treatments  $\geq 1140 \mu\text{atm}$ .

ergy requirements for these alternate pathways have been demonstrated, where measurements of maximum photosynthetic rates ( $P_{\text{max}}$ ) and photosynthetic efficiency ( $\alpha$ ) display changes that result in no change to saturating irradiance levels ( $E_k$ ) (Behrenfeld et al., 2004, 2008; Halsey et al., 2010). This “ $E_k$ -independent variability” was evident in our study, in which decreases in  $P_{\text{max}}$  and  $\alpha$  were observed in the high  $\text{CO}_2$  treatments, while  $E_k$  remained unaffected (Fig. S3 in the Supplement).

This highlights an important tipping point in the phytoplankton community’s ability to cope with the energetic requirements of maintaining efficient productivity under high  $\text{CO}_2$ . While studies on individual phytoplankton species have reported decoupling of the photosynthetic pathway under conditions of stress, no studies to date on natural phytoplankton communities have reported this response. Under laboratory conditions, stresses such as nutrient limitations (Halsey et al., 2010) or a combination of high  $\text{CO}_2$  and light climate (Hoppe et al., 2015; Liu et al., 2017) have been shown to induce such a response in which isolated phytoplankton species possess higher energy requirements for carbon fixation. In our study, the phytoplankton community experienced a dynamic light climate due to continuous gentle mixing of the minicosm contents, and although nutrients were not limiting, the phytoplankton in the higher  $\text{CO}_2$  treatments did show lower  $\text{csGPP}_{14\text{C}}$  rates (Fig. 6a), which could be linked to higher energy demand for light-independent processes. Since nutrients were replete and not a likely source of stress, it follows that  $\text{CO}_2$  and light were likely the only sources of stress on this community.

Increased respiration rates could account for the decreased carbon fixation rates measured. Thus far, respiration rates are commonly reported as either unaffected or lower under increasing  $\text{CO}_2$  (Hennon et al., 2014; Trimbom et al., 2014; Spilling et al., 2016). This effect is generally attributed to de-

clines in cellular energy requirements via processes such as the down-regulation of CCMs, which can result in observed increased rates of production (Spilling et al., 2016). Despite this, decreased growth rates have been linked to enhanced respiratory carbon loss at high  $\text{CO}_2$  levels (800–1000  $\mu\text{atm}$ ) (Gao et al., 2012b). The contribution of community respiration rates to  $\text{csGCP}_{\text{O}_2}$  was high and increased with increasing  $\text{CO}_2$  (Fig. S4 in the Supplement). However, respiration rates were generally proportional to the increase in  $\text{O}_2$  production (i.e. the ratio of production to respiration remained constant across  $\text{CO}_2$  conditions), making it unlikely to be a significant contributor to the decline in carbon fixation. Instead, high respiration rates were possibly a result of heterotrophic activity.

It has been suggested that the negative effects of ocean acidification are predominantly due to the decline in pH and not the increase in  $\text{CO}_2$  concentration (e.g. McMinn et al., 2014; Coad et al., 2016). A decline in pH with ocean acidification increases the hydrogen ion ( $\text{H}^+$ ) concentration in the seawater and is likely to make it increasingly difficult for phytoplankton cells to maintain cellular homeostasis. Metabolic processes, such as photosynthesis and respiration, impact cellular  $\text{H}^+$  fluxes between compartments, making it necessary to temporarily balance internal  $\text{H}^+$  concentrations through  $\text{H}^+$  channels (Taylor et al., 2012). Under normal oceanic conditions (pH  $\sim 8.1$ ), when the extracellular environment is above pH 7.8, excess  $\text{H}^+$  ions generated within the cell are able to passively diffuse out of the cell through these  $\text{H}^+$  channels. However, a lowering of the oceanic pH below 7.8 is likely to halt this passive removal of internal  $\text{H}^+$ , requiring the utilisation of energy-intensive proton pumps (Taylor et al., 2012) and thus potentially reducing the energy pool available for carbon fixation. While not well understood, these  $\text{H}^+$  channels may also perform important cellular functions, such as nutrient uptake, cellular signalling,

and defense (Taylor et al., 2012). Our results are consistent with this idea of a critical pH threshold, as significant declines in  $GPP_{14C}$  were observed in treatments  $\geq 1140 \mu\text{atm}$  (Fig. 10), which are the  $\text{CO}_2$  treatments for which the pH ranged from 7.69–7.45 (Fig. 2).

Despite the initial stress of high  $\text{CO}_2$  between days 8 and 12, the phytoplankton community displayed a strong ability to adapt to these conditions. The  $\text{CO}_2$ -induced reduction in  $F_v / F_m$  showed a steady recovery between days 12 and 16, with all treatments displaying similarly high  $F_v / F_m$  at day 16 (0.68–0.71; Fig. 7). This recovery in photosynthetic health suggests that the phytoplankton community was able to acclimate to the high  $\text{CO}_2$  conditions, possibly through cellular acclimation, changes in community structure, or most likely, a combination of both. Cellular acclimations were observed in our study. A lowering of NPQ and a minimisation of the  $\text{CO}_2$ -related response to photoinhibition (rETR) at high light intensity suggested that PSII was being down-regulated to adjust to a higher light climate (Figs. S6 and S7 in the Supplement). Decreased energy requirements for carbon fixation were also observed in the photosynthetic pathway, resulting in increases in  $GPP_{14C}$  and Chl *a* accumulation rates (Fig. 5). Acclimation to increased  $\text{CO}_2$  has been reported in a number of studies, resulting in shifts in carbon and energy utilisation (Sobrino et al., 2008; Hopkinson et al., 2010; Hennon et al., 2014; Trimborn et al., 2014; Zheng et al., 2015). Numerous photophysiological investigations on individual phytoplankton species also report species-specific tolerances to increased  $\text{CO}_2$  (Gao et al., 2012a; Gao and Campbell, 2014; Trimborn et al., 2013, 2014), and a general trend toward smaller-celled communities with increased  $\text{CO}_2$  has been reported in ocean acidification studies globally (Schulz et al., 2017). Changes in community structure were observed with increasing  $\text{CO}_2$ , with taxon-specific thresholds of  $\text{CO}_2$  tolerance (Hancock et al., 2017). Within the diatom community, the response was also related to size, leading to an increase in abundance of small ( $< 20 \mu\text{m}$ ) diatoms in the higher  $\text{CO}_2$  treatments ( $\geq 953 \mu\text{atm}$ ). Therefore, the community acclimation observed is likely driven by an increase in the growth of more tolerant species.

It is often suggested that the down-regulation of CCMs helps to moderate the sensitivity of phytoplankton communities to increasing  $\text{CO}_2$ . The carbon-fixing enzyme Ru-BisCO has a low affinity for  $\text{CO}_2$  that is compensated for through CCMs that actively increase the intracellular  $\text{CO}_2$  (Raven, 1991; Badger, 1994; Badger et al., 1998; Hopkinson et al., 2011). This process requires additional cellular energy (Raven, 1991) and numerous studies have suggested that the energy savings from down-regulation of CCMs in phytoplankton could explain increases in rates of primary productivity at elevated  $\text{CO}_2$  levels (e.g. Cassar et al., 2004; Tortell et al., 2008b, 2010; Trimborn et al., 2013; Young et al., 2015). In Antarctic phytoplankton communities, Young et al. (2015) showed that the energetic costs of CCMs are low and any down-regulation at increased  $\text{CO}_2$  would provide little

benefit. We found that the CCM component carbonic anhydrase (CA) was utilised by the phytoplankton community at our control  $\text{CO}_2$  level (343  $\mu\text{atm}$ ) and was down-regulated at high  $\text{CO}_2$  (1641  $\mu\text{atm}$ ; Fig. 8). Yet we saw no promotion of primary productivity that coincided with this down-regulation. Thus, our data support the previous studies showing that increased  $\text{CO}_2$  may alleviate energy supply constraints but does not necessarily lead to increased rates of carbon fixation (Rost et al., 2003; Cassar et al., 2004; Riebesell, 2004).

Furthermore, size-specific differences in phytoplankton CCM utilisation were observed. The absence of eCA activity in the large phytoplankton ( $\geq 10 \mu\text{m}$ ; Fig. 8a) suggests that bicarbonate ( $\text{HCO}_3^-$ ) was the dominant carbon source used by this fraction of the phytoplankton community (Burkhardt et al., 2001; Tortell et al., 2008a). This is not surprising as direct  $\text{HCO}_3^-$  uptake has been commonly reported among Antarctic phytoplankton communities (Cassar et al., 2004; Tortell et al., 2008a, 2010). On the other hand, the small phytoplankton ( $< 10 \mu\text{m}$ ; Fig. 8b) seem to have used both iCA and eCA, implying that carbon for photosynthesis was sourced through both the extracellular conversion of  $\text{HCO}_3^-$  to  $\text{CO}_2$  and direct  $\text{HCO}_3^-$  uptake (Rost et al., 2003). Despite these patterns, CCM activity in this study was only determined via Chl *a* fluorescence and therefore direct measurement of light-dependent reactions in photosynthesis. This imposes limitations to the interpretability of this particular data set, as CA is involved primarily in carbon acquisition, which occurs during photosynthetic reactions that are independent of light.

The presence of iCA has also been proposed as a possible mechanism for increased sensitivity of phytoplankton to decreased pH conditions. Satoh et al. (2001) found that the presence of iCA caused strong intracellular acidification and inhibition of carbon fixation when a  $\text{CO}_2$ -tolerant iCA-expressing algal species was transferred from ambient conditions to very high  $\text{CO}_2$  (40 %). Down-regulation of iCA through acclimation in a 5 %  $\text{CO}_2$  treatment eliminated this response, with similar tolerance observed in an algal species with low ambient iCA activity. Thus, the down-regulation of iCA activity at high  $\text{CO}_2$ , as was seen in our study, may not only decrease cellular energy demands but may also be operating as a cellular protection mechanism, allowing the cell to maintain intracellular homeostasis.

Contrary to the high  $\text{CO}_2$  treatments, the phytoplankton community appeared to tolerate  $\text{CO}_2$  levels up to 953  $\mu\text{atm}$ , which identified a  $\text{CO}_2$  threshold. Between days 8 and 14 we observed a small and insignificant  $\text{CO}_2$ -related decline in  $F_v / F_m$ ,  $GPP_{14C}$ , and Chl *a* accumulation among the 343–953  $\mu\text{atm}$  treatments (Figs. 7 and 10). Tolerance of  $\text{CO}_2$  levels up to  $\sim 1000 \mu\text{atm}$  has often been observed in natural phytoplankton communities in regions exposed to fluctuating  $\text{CO}_2$  levels. In these communities, increasing  $\text{CO}_2$  often had no effect on primary productivity (Tortell et al., 2000; Tortell and Morel, 2002; Tortell et al., 2008b; Hopkinson

et al., 2010; Tanaka et al., 2013; Sommer et al., 2015; Young et al., 2015; Spilling et al., 2016) or growth (Tortell et al., 2008b; Schulz et al., 2013), although an increase in primary production has been observed in some instances (Riebesell, 2004; Tortell et al., 2008b; Egge et al., 2009; Tortell et al., 2010; Hoppe et al., 2013; Holding et al., 2015). These differing responses may be due to differences in community composition, nutrient supply, or ecological adaptations of the phytoplankton community in the region studied. They may also be due to differences in the experimental methods, especially the range of CO<sub>2</sub> concentrations employed (Hancock et al., 2017), the mechanism used to manipulate CO<sub>2</sub> concentrations, the duration of the acclimation and incubation, the nature and volume of the mesocosms used, and the extent to which higher trophic levels are screened from the mesocosm contents (see Davidson et al., 2016).

Previous studies in Prydz Bay report a tolerance of the phytoplankton community to CO<sub>2</sub> levels up to 750 μatm (Davidson et al., 2016; Thomson et al., 2016; Westwood et al., 2018). Although these experiments differed in nutrient concentration, community composition, and CO<sub>2</sub> manipulation from ours, when taken together, these studies demonstrate consistent CO<sub>2</sub> effects throughout the Antarctic summer season and across years in this location. The most likely reason for this high tolerance is that these communities are already exposed to highly variable CO<sub>2</sub> conditions. CO<sub>2</sub> naturally builds beneath the sea ice in winter when primary productivity is low (Perrin et al., 1987; Legendre et al., 1992), and is rapidly depleted during spring and summer by phytoplankton blooms, resulting in annual *f*CO<sub>2</sub> fluctuations between ~50 and 500 μatm (Gibson and Trull, 1999; Roden et al., 2013). Thus, variable CO<sub>2</sub> environments appear to promote adaptations within the phytoplankton community to manage the stress imposed by fluctuating CO<sub>2</sub>.

Changes in POM production and the C:N ratio in phytoplankton communities can have significant effects on carbon sequestration and change their nutritional value for higher trophic levels (Finkel et al., 2010; van de Waal et al., 2010; Polimene et al., 2016). We observed a decline in particulate organic matter production (POM) at CO<sub>2</sub> levels ≥ 1140 μatm (Fig. 10), while changes in organic matter stoichiometry (C:N ratio) appeared to be predominantly controlled by nutrient consumption (Fig. 4). Increases in POM production were similar to Chl *a* accumulation, with declines in high CO<sub>2</sub> treatments (≥ 1140 μatm) due to low rates of primary productivity. Carbon overconsumption has been reported in some natural phytoplankton communities exposed to increased CO<sub>2</sub>, resulting in observed or inferred increases in the particulate C:N ratio (Riebesell et al., 2007; Engel et al., 2014). While in our study the C:N ratio did decline to below the Redfield ratio during exponential growth, it remained within previously reported C:N ratios of coastal phytoplankton communities in this region (Gibson and Trull, 1999; Pasquer et al., 2010). However, as we did not analyse the elemental composition of dissolved inorganic matter, car-

bon overconsumption cannot be completely ruled out (Kähler and Koeve, 2001). Therefore, it is difficult to say whether or not changes in primary productivity will affect organic matter stoichiometry in this region, particularly as any resultant long-term changes in community composition to more CO<sub>2</sub>-tolerant taxa may also have an effect (Finkel et al., 2010).

#### 4.2 Ocean acidification effects on bacterial productivity

In contrast to the phytoplankton community, bacteria were tolerant of high CO<sub>2</sub> levels. The low bacterial productivity and abundance of the initial community is characteristic of the post-winter bacterial community in Prydz Bay where growth is limited by organic nutrient availability (Pearce et al., 2007). Whilst an increase in cell abundance was observed at CO<sub>2</sub> levels ≥ 634 μatm (Fig. 9a), it was possible that this response was driven by a decline in grazing by heterotrophs (Thomson et al., 2016; Westwood et al., 2018) instead of a direct CO<sub>2</sub>-related promotion of bacterial growth. The subsequent decline in abundance was likely due to top-down control from the heterotrophic nanoflagellate community, which displayed an increase in abundance at this time (Hancock et al., 2017). Bacterial tolerance to high CO<sub>2</sub> has been reported previously in this region (Thomson et al., 2016; Westwood et al., 2018) and has also been reported in numerous studies in the Arctic (Grossart et al., 2006; Allgaier et al., 2008; Paulino et al., 2008; Baragi et al., 2015; Wang et al., 2016), suggesting that the marine bacterial community will be resilient to increasing CO<sub>2</sub>.

While we detected an increase in bacterial productivity, this response appeared to be correlated with an increase in Chl *a* concentration and available POM rather than CO<sub>2</sub>. Bacterial productivity was similar among all CO<sub>2</sub> treatments, except for a final promotion of productivity at 634 μatm on day 18 (Fig. 9b). This promotion of growth may be linked to an increase in diatom abundance observed in this treatment (Hancock et al., 2017). The coupling of bacterial growth with phytoplankton productivity has been reported by numerous studies on natural marine microbial communities (Allgaier et al., 2008; Grossart et al., 2006; Engel et al., 2013; Piontek et al., 2013; Sperling et al., 2013; Bergen et al., 2016). Thus, it is likely that the bacterial community was controlled more by grazing and nutrient availability than by CO<sub>2</sub> level.

## 5 Conclusions

These results support the identification of a tipping point in the marine microbial community response to CO<sub>2</sub> between 953 and 1140 μatm. When exposed to CO<sub>2</sub> ≥ 634 μatm, declines in growth rates, primary productivity, and organic matter production were observed in the phytoplankton community and became significantly different at ≥ 1140 μatm. Despite this, the community displayed the ability to adapt to these high CO<sub>2</sub> conditions by down-regulating CCMs and



likely adjusting other intracellular mechanisms to cope with the added stress of low pH. However, the lag in growth and subsequent acclimation to high CO<sub>2</sub> conditions allowed for more tolerant species to thrive (Hancock et al., 2017).

Conditions in Antarctic coastal regions fluctuate throughout the seasons and the marine microbial community is already tolerant to changes in CO<sub>2</sub> level, light availability, and nutrients (Gibson and Trull, 1999; Roden et al., 2013). It is possible that phytoplankton communities already exposed to highly variable conditions will be more capable of adapting to the projected changes in CO<sub>2</sub> (Schaum and Collins, 2014; Boyd et al., 2016). This will likely also include adaptation at the community level, causing a shift in dominance to more tolerant species. This has been observed in numerous ocean acidification experiments, with a trend in community composition favouring picophytoplankton and away from large diatoms (Davidson et al., 2016; reviewed in Schulz et al., 2017). Such a change in phytoplankton community composition may have flow-on effects to higher trophic levels that feed on Antarctic phytoplankton blooms. It could also have a significant effect on the biological pump, with decreased carbon drawdown at high CO<sub>2</sub>, causing a negative feedback on anthropogenic CO<sub>2</sub> uptake. Coincident increases in bacterial abundance under high CO<sub>2</sub> conditions may also increase the efficiency of the microbial loop, resulting in increased organic matter remineralisation and further declines in carbon sequestration.

*Data availability.* Experimental data used for analysis are available via the Australian Antarctic Data Centre.

Environmental data: Australian Antarctic Data Centre, <http://dx.doi.org/10.4225/15/599a7dfe9470a> (Deppeler et al., 2017a).

Productivity data: Australian Antarctic Data Centre, <http://dx.doi.org/10.4225/15/599a7cc747c61> (Deppeler et al., 2017b).

**The Supplement related to this article is available online at <https://doi.org/10.5194/bg-15-209-2018-supplement>.**

*Author contributions.* AD, KW, and KP conceived and designed the experiments. AD led and oversaw the minicosm experiment. SD and KP performed the experiments and data analysis. KS performed the carbonate system measurements and manipulation. IP performed pigment extraction and analysis. JM provided statistical guidance. SD wrote the paper with significant input from KP, KS, and AD. All authors provided contributions and a critical review of the paper.

*Competing interests.* The authors declare that they have no conflict of interest.

*Acknowledgements.* This study was funded by the Australian Government, Department of Environment and Energy as part of the Australian Antarctic Science Project 4026 at the Australian Antarctic Division and an Elite Research Scholarship awarded by the Institute for Marine and Antarctic Studies, University of Tasmania. We would like to thank Andrew McMinn for valuable comments on our paper, Penelope Pascoe for the flow cytometric analyses, Cristin Sheehan for photosynthesis and respiration data, and Thomas Rodemann from the Central Science Laboratory, University of Tasmania for elemental analysis of our POM samples. We gratefully acknowledge the assistance of AAD technical support in designing and equipping the minicosms and Davis Station expeditioners in the summer of 2014–2015 for their support and assistance.

Edited by: Richard Matear

Reviewed by: two anonymous referees

## References

- Allgaier, M., Riebesell, U., Vogt, M., Thyraug, R., and Grossart, H.-P.: Coupling of heterotrophic bacteria to phytoplankton bloom development at different pCO<sub>2</sub> levels: a mesocosm study, *Biogeosciences*, 5, 1007–1022, <https://doi.org/10.5194/bg-5-1007-2008>, 2008.
- Arrigo, K. R., van Dijken, G. L., and Bushinsky, S.: Primary production in the Southern Ocean, 1997–2006, *J. Geophys. Res.-Ocean.*, 113, C08004, <https://doi.org/10.1029/2007JC004551>, 2008a.
- Arrigo, K. R., van Dijken, G. L., and Long, M.: Coastal Southern Ocean: A strong anthropogenic CO<sub>2</sub> sink, *Geophys. Res. Lett.*, 35, L21602, <https://doi.org/10.1029/2008GL035624>, 2008b.
- Azam, F., Fenchel, T., Field, J. G., Gray, J. C., Meyer-Reil, L. A., and Thingstad, F.: The ecological role of water-column microbes in the sea, *Mar. Ecol. Prog. Ser.*, 10, 257–264, <https://doi.org/10.3354/meps010257>, 1983.
- Azam, F., Smith, D. C., and Hollibaugh, J. T.: The role of the microbial loop in Antarctic pelagic ecosystems, *Polar Res.*, 10, 239–243, <https://doi.org/10.1111/j.1751-8369.1991.tb00649.x>, 1991.
- Bach, L. T., Taucher, J., Boxhammer, T., Ludwig, A., Achterberg, E. P., Algueró-Muñiz, M., Anderson, L. G., Bellworthy, J., Büdenbender, J., Czerny, J., Ericson, Y., Esposito, M., Fischer, M., Haunost, M., Hellemann, D., Horn, H. G., Hornick, T., Meyer, J., Sswat, M., Zark, M., and Riebesell, U.: Influence of ocean acidification on a natural winter-to-summer plankton succession first insights from a long-term mesocosm study draw attention to periods of low nutrient concentrations, *PLoS One*, 11, e0159068, <https://doi.org/10.1371/journal.pone.0159068>, 2016.
- Badger, M.: The Role of Carbonic Anhydrase in Photosynthesis, *Annu. Rev. Plant Physiol. Plant Mol. Biol.*, 45, 369–392, <https://doi.org/10.1146/annurev.arplant.45.1.369>, 1994.
- Badger, M. R., Andrews, T. J., Whitney, S., Ludwig, M., Yellowlees, D. C., Leggat, W., and Price, G. D.: The diversity and coevolution of Rubisco, plastids, pyrenoids, and chloroplast-based CO<sub>2</sub>-concentrating mechanisms in algae, *Can. J. Bot.*, 76, 1052–1071, <https://doi.org/10.1139/cjb-76-6-1052>, 1998.
- Baragi, L. V., Khandeparker, L., and Anil, A. C.: Influence of elevated temperature and pCO<sub>2</sub> on the marine periphytic diatom

- Navicula distans* and its associated organisms in culture, *Hydrobiologia*, 762, 127–142, <https://doi.org/10.1007/s10750-015-2343-9>, 2015.
- Barcelos e Ramos, J., Schulz, K. G., Brownlee, C., Sett, S., and Azevedo, E. B.: Effects of Increasing Seawater Carbon Dioxide Concentrations on Chain Formation of the Diatom *Asterionellopsis glacialis*, *PLoS One*, 9, e90749, <https://doi.org/10.1371/journal.pone.0090749>, 2014.
- Behrenfeld, M. J., Prasil, O., Babin, M., and Bruyant, F.: In Search of a Physiological Basis for Covariations in Light-Limited and Light-Saturated Photosynthesis, *J. Phycol.*, 40, 4–25, <https://doi.org/10.1046/j.1529-8817.2004.03083.x>, 2004.
- Behrenfeld, M. J., Halsey, K. H., and Milligan, A. J.: Evolved physiological responses of phytoplankton to their integrated growth environment., *Philos. T. R. Soc. B*, 363, 2687–2703, <https://doi.org/10.1098/rstb.2008.0019>, 2008.
- Bellerby, R. G. J., Schulz, K. G., Riebesell, U., Neill, C., Nondal, G., Heegaard, E., Johannessen, T., and Brown, K. R.: Marine ecosystem community carbon and nutrient uptake stoichiometry under varying ocean acidification during the PeECE III experiment, *Biogeosciences*, 5, 1517–1527, <https://doi.org/10.5194/bg-5-1517-2008>, 2008.
- Berge, T., Daugbjerg, N., Balling Andersen, B., and Hansen, P.: Effect of lowered pH on marine phytoplankton growth rates, *Mar. Ecol. Prog. Ser.*, 416, 79–91, <https://doi.org/10.3354/meps08780>, 2010.
- Bergen, B., Endres, S., Engel, A., Zark, M., Dittmar, T., Sommer, U., and Jürgens, K.: Acidification and warming affect prominent bacteria in two seasonal phytoplankton bloom mesocosms, *Environ. Microbiol.*, 18, 4579–4595, <https://doi.org/10.1111/1462-2920.13549>, 2016.
- Bi, R., Ismar, S., Sommer, U., and Zhao, M.: Environmental dependence of the correlations between stoichiometric and fatty acid-based indicators of phytoplankton nutritional quality, *Limnol. Oceanogr.*, 62, 334–347, <https://doi.org/10.1002/lno.10429>, 2017.
- Bockmon, E. E. and Dickson, A. G.: A seawater filtration method suitable for total dissolved inorganic carbon and pH analyses, *Limnol. Oceanogr. Methods*, 12, 191–195, <https://doi.org/10.4319/lom.2014.12.191>, 2014.
- Boyd, P. W., Doney, S. C., Strzepek, R., Dusenberry, J., Lindsay, K., and Fung, I.: Climate-mediated changes to mixed-layer properties in the Southern Ocean: assessing the phytoplankton response, *Biogeosciences*, 5, 847–864, <https://doi.org/10.5194/bg-5-847-2008>, 2008.
- Boyd, P. W., Cornwall, C. E., Davidson, A., Doney, S. C., Fourquez, M., Hurd, C. L., Lima, I. D., and McMinn, A.: Biological responses to environmental heterogeneity under future ocean conditions, *Global Change Biol.*, 22, 2633–2650, <https://doi.org/10.1111/gcb.13287>, 2016.
- Bunse, C., Lundin, D., Karlsson, C. M. G., Vila-Costa, M., Palo-vaara, J., Akram, N., Svensson, L., Holmfeldt, K., González, J. M., Calvo, E., Pelejero, C., Marrasé, C., Dopson, M., Gasol, J. M., and Pinhassi, J.: Response of marine bacterioplankton pH homeostasis gene expression to elevated CO<sub>2</sub>, *Nat. Clim. Change*, 1, 1–7, <https://doi.org/10.1038/nclimate2914>, 2016.
- Burkhardt, S., Amoroso, G., Riebesell, U., and Sültemeyer, D.: CO<sub>2</sub> and HCO<sub>3</sub><sup>-</sup> uptake in marine diatoms acclimated to different CO<sub>2</sub> concentrations, *Limnol. Oceanogr.*, 46, 1378–1391, <https://doi.org/10.4319/lo.2001.46.6.1378>, 2001.
- Caldeira, K. and Wickett, M. E.: Oceanography: Anthropogenic carbon and ocean pH, *Nature*, 425, 365–365, <https://doi.org/10.1038/425365a>, 2003.
- Cassar, N., Laws, E. A., Bidigare, R. R., and Popp, B. N.: Bicarbonate uptake by Southern Ocean phytoplankton, *Global Biogeochem. Cy.*, 18, 1–10, <https://doi.org/10.1029/2003GB002116>, 2004.
- Chen, C. and Durbin, E.: Effects of pH on the growth and carbon uptake of marine phytoplankton, *Mar. Ecol. Prog. Ser.*, 109, 83–94, <https://doi.org/10.3354/meps109083>, 1994.
- Chen, H., Guan, W., Zeng, G., Li, P., and Chen, S.: Alleviation of solar ultraviolet radiation (UVR)-induced photoinhibition in diatom *Chaetoceros curvisetus* by ocean acidification, *J. Mar. Biol. Assoc. UK*, 95, 661–667, <https://doi.org/10.1017/S0025315414001568>, 2015.
- Coad, T., McMinn, A., Nomura, D., and Martin, A.: Effect of elevated CO<sub>2</sub> concentration on microalgal communities in Antarctic pack ice, *Deep-Sea Res. Part II*, 131, 160–169, <https://doi.org/10.1016/j.dsr2.2016.01.005>, 2016.
- Davidson, A., McKinlay, J., Westwood, K., Thomson, P., van den Enden, R., de Salas, M., Wright, S., Johnson, R., and Berry, K.: Enhanced CO<sub>2</sub> concentrations change the structure of Antarctic marine microbial communities, *Mar. Ecol. Prog. Ser.*, 552, 93–113, <https://doi.org/10.3354/meps11742>, 2016.
- Deppeler, S. L. and Davidson, A. T.: Southern Ocean Phytoplankton in a Changing Climate, *Front. Mar. Sci.*, 4, 1–28, <https://doi.org/10.3389/fmars.2017.00040>, 2017.
- Deppeler, S. L., Davidson, A. T., and Schulz, K.: Environmental data for Davis 14/15 ocean acidification minicosm experiment, Australian Antarctic Data Centre, <https://doi.org/10.4225/15/599a7dfe9470a>, 2017a (updated 2017).
- Deppeler, S. L., Petrou, K., Schulz, K., Davidson, A. T., McKinlay, J., Pearce, I., and Westwood, K. J.: Data for manuscript “Ocean acidification of a coastal Antarctic marine microbial community reveals a critical threshold for CO<sub>2</sub> tolerance in phytoplankton productivity”, Australian Antarctic Data Centre, <https://doi.org/10.4225/15/599a7cc747c61>, 2017b (updated 2017).
- Dickson, A.: Standards for Ocean Measurements, *Oceanography*, 23, 34–47, <https://doi.org/10.5670/oceanog.2010.22>, 2010.
- Dickson, A., Sabine, C., and Christian, J., eds.: Guide to Best Practices for Ocean CO<sub>2</sub> Measurements, North Pacific Marine Science Organization, Sidney, British Columbia, 191 pp., 2007.
- Dring, M. J. and Jewson, D. H.: What Does 14C Uptake by Phytoplankton Really Measure? A Theoretical Modelling Approach, *Proc. R. Soc. B*, 214, 351–368, <https://doi.org/10.1098/rspb.1982.0016>, 1982.
- Ducklow, H. W., Baker, K., Martinson, D. G., Quetin, L. B., Ross, R. M., Smith, R. C., Stammerjohn, S. E., Vernet, M., and Fraser, W.: Marine pelagic ecosystems: the West Antarctic Peninsula, *Philos. T. R. Soc. B*, 362, 67–94, <https://doi.org/10.1098/rstb.2006.1955>, 2007.
- EGge, J. K., Thingstad, T. F., Larsen, A., Engel, A., Wohlers, J., Bellerby, R. G. J., and Riebesell, U.: Primary production during nutrient-induced blooms at elevated CO<sub>2</sub> concentrations,

- Biogeosciences, 6, 877–885, <https://doi.org/10.5194/bg-6-877-2009>, 2009.
- Engel, A., Borchard, C., Piontek, J., Schulz, K. G., Riebesell, U., and Bellerby, R.: CO<sub>2</sub> increases <sup>14</sup>C primary production in an Arctic plankton community, *Biogeosciences*, 10, 1291–1308, <https://doi.org/10.5194/bg-10-1291-2013>, 2013.
- Engel, A., Piontek, J., Grossart, H.-P., Riebesell, U., Schulz, K. G., and Sperling, M.: Impact of CO<sub>2</sub> enrichment on organic matter dynamics during nutrient induced coastal phytoplankton blooms, *J. Plankton Res.*, 36, 641–657, <https://doi.org/10.1093/plankt/fbt125>, 2014.
- Fabry, V., McClintock, J., Mathis, J., and Grebmeier, J.: Ocean Acidification at High Latitudes: The Bellwether, *Oceanography*, 22, 160–171, <https://doi.org/10.5670/oceanog.2009.105>, 2009.
- Fenchel, T.: The microbial loop – 25 years later, *J. Exp. Mar. Bio. Ecol.*, 366, 99–103, <https://doi.org/10.1016/j.jembe.2008.07.013>, 2008.
- Feng, Y., Hare, C., Rose, J., Handy, S., DiTullio, G., Lee, P., Smith, W. J., Peloquin, J., Tozzi, S., Sun, J., Zhang, Y., Dunbar, R., Long, M., Sohst, B., Lohan, M., and Hutchins, D.: Interactive effects of iron, irradiance and CO<sub>2</sub> on Ross Sea phytoplankton, *Deep-Sea Res. Part I*, 57, 368–383, <https://doi.org/10.1016/j.dsr.2009.10.013>, 2010.
- Finkel, Z. V., Beardall, J., Flynn, K. J., Quigg, A., Rees, T. A. V., and Raven, J. A.: Phytoplankton in a changing world: cell size and elemental stoichiometry, *J. Plankton Res.*, 32, 119–137, <https://doi.org/10.1093/plankt/fbp098>, 2010.
- Frölicher, T. L., Sarmiento, J. L., Paynter, D. J., Dunne, J. P., Krasting, J. P., and Winton, M.: Dominance of the Southern Ocean in Anthropogenic Carbon and Heat Uptake in CMIP5 Models, *J. Clim.*, 28, 862–886, <https://doi.org/10.1175/JCLI-D-14-00117.1>, 2015.
- Gao, K. and Campbell, D. A.: Photophysiological responses of marine diatoms to elevated CO<sub>2</sub> and decreased pH: a review, *Funct. Plant Biol.*, 41, 449–459, <https://doi.org/10.1071/FP13247>, 2014.
- Gao, K., Helbling, E., Häder, D., and Hutchins, D.: Responses of marine primary producers to interactions between ocean acidification, solar radiation, and warming, *Mar. Ecol. Prog. Ser.*, 470, 167–189, <https://doi.org/10.3354/meps10043>, 2012a.
- Gao, K., Xu, J., Gao, G., Li, Y., Hutchins, D. A., Huang, B., Wang, L., Zheng, Y., Jin, P., Cai, X., Häder, D.-p., Li, W., Xu, K., Liu, N., and Riebesell, U.: Rising CO<sub>2</sub> and increased light exposure synergistically reduce marine primary productivity, *Nat. Clim. Change*, 2, 519–523, <https://doi.org/10.1038/nclimate1507>, 2012b.
- Gattuso, J.-P., Gao, K., Lee, K., Rost, B., and Schulz, K. G.: Approaches and tools to manipulate the carbonate chemistry, in: Guide to best practices for ocean acidification research and data reporting, edited by Riebesell, U., Fabry, V. J., Hansson, L., and Gattuso, J.-P., chap. 2, 41–52, Publications Office of the European Union, Luxembourg, <https://doi.org/10.2777/66906>, 2010.
- Gibson, J. A. and Trull, T. W.: Annual cycle of *f*CO<sub>2</sub> under sea-ice and in open water in Prydz Bay, East Antarctica, *Mar. Chem.*, 66, 187–200, [https://doi.org/10.1016/S0304-4203\(99\)00040-7](https://doi.org/10.1016/S0304-4203(99)00040-7), 1999.
- González, N., Gattuso, J. P., and Middelburg, J. J.: Oxygen production and carbon fixation in oligotrophic coastal bays and the relationship with gross and net primary production, *Aquat. Microb. Ecol.*, 52, 119–130, <https://doi.org/10.3354/ame01208>, 2008.
- Grossart, H.-P., Allgaier, M., Passow, U., and Riebesell, U.: Testing the effect of CO<sub>2</sub> concentration on the dynamics of marine heterotrophic bacterioplankton, *Limnol. Oceanogr.*, 51, 1–11, <https://doi.org/10.4319/lo.2006.51.1.0001>, 2006.
- Halsey, K. H., Milligan, A. J., and Behrenfeld, M. J.: Physiological optimization underlies growth rate-independent chlorophyll-specific gross and net primary production, *Photosynth. Res.*, 103, 125–137, <https://doi.org/10.1007/s11120-009-9526-z>, 2010.
- Hancock, A. M., Davidson, A. T., McKinlay, J., McMinn, A., Schulz, K., and van den Enden, R. L.: Ocean acidification changes the structure of an Antarctic coastal protistan community, *Biogeosciences Discuss.*, <https://doi.org/10.5194/bg-2017-224>, in review, 2017.
- Hauck, J. and Völker, C.: Rising atmospheric CO<sub>2</sub> leads to large impact of biology on Southern Ocean CO<sub>2</sub> uptake via changes of the Revelle factor, *Geophys. Res. Lett.*, 42, 1459–1464, <https://doi.org/10.1002/2015GL063070>, 2015.
- Hauck, J., Völker, C., Wolf-Gladrow, D. A., Laufkötter, C., Vogt, M., Aumont, O., Bopp, L., Buitenhuis, E. T., Doney, S. C., Dunne, J., Gruber, N., Hashioka, T., John, J., Quéré, C. L., Lima, I. D., Nakano, H., Séférian, R., and Totterdell, I.: On the Southern Ocean CO<sub>2</sub> uptake and the role of the biological carbon pump in the 21st century, *Global Biogeochem. Cy.*, 29, 1451–1470, <https://doi.org/10.1002/2015GB005140>, 2015.
- Hennon, G. M. M., Quay, P., Morales, R. L., Swanson, L. M., and Virginia Armbrust, E.: Acclimation conditions modify physiological response of the diatom *Thalassiosira pseudonana* to elevated CO<sub>2</sub> concentrations in a nitrate-limited chemostat, *J. Phycol.*, 50, 243–253, <https://doi.org/10.1111/jpy.12156>, 2014.
- Hennon, G. M. M., Ashworth, J., Groussman, R. D., Berthiaume, C., Morales, R. L., Baliga, N. S., Orellana, M. V., and Armbrust, E. V.: Diatom acclimation to elevated CO<sub>2</sub> via cAMP signalling and coordinated gene expression, *Nat. Clim. Change*, 5, 761–765, <https://doi.org/10.1038/nclimate2683>, 2015.
- Holding, J. M., Duarte, C. M., Sanz-Martín, M., Mesa, E., Arrieta, J. M., Chierici, M., Hendriks, I. E., García-Corral, L. S., Regaudie-de Gioux, A., Delgado, A., Reigstad, M., Wassmann, P., and Agustí, S.: Temperature dependence of CO<sub>2</sub>-enhanced primary production in the European Arctic Ocean, *Nat. Clim. Change*, 5, 1079–1082, <https://doi.org/10.1038/nclimate2768>, 2015.
- Hong, H., Li, D., Lin, W., Li, W., and Shi, D.: Nitrogen nutritional condition affects the response of energy metabolism in diatoms to elevated carbon dioxide, *Mar. Ecol. Prog. Ser.*, 567, 41–56, <https://doi.org/10.3354/meps12033>, 2017.
- Honjo, S.: Particle export and the biological pump in the Southern Ocean, *Antarct. Sci.*, 16, 501–516, <https://doi.org/10.1017/S0954102004002287>, 2004.
- Hopkinson, B. M., Xu, Y., Shi, D., McGinn, P. J., and Morel, F. M. M.: The effect of CO<sub>2</sub> on the photosynthetic physiology of phytoplankton in the Gulf of Alaska, *Limnol. Oceanogr.*, 55, 2011–2024, <https://doi.org/10.4319/lo.2010.55.5.2011>, 2010.
- Hopkinson, B. M., Dupont, C. L., Allen, A. E., and Morel, F. M. M.: Efficiency of the CO<sub>2</sub>-concentrating mechanism of diatoms, *P. Natl. Acad. Sci.*, 108, 3830–3837, <https://doi.org/10.1073/pnas.1018062108>, 2011.

- Hoppe, C. J. M., Hassler, C. S., Payne, C. D., Tortell, P. D., Rost, B., and Trimborn, S.: Iron Limitation Modulates Ocean Acidification Effects on Southern Ocean Phytoplankton Communities, *PLoS One*, 8, e79890, <https://doi.org/10.1371/journal.pone.0079890>, 2013.
- Hoppe, C. J. M., Holtz, L.-M., Trimborn, S., and Rost, B.: Ocean acidification decreases the light-use efficiency in an Antarctic diatom under dynamic but not constant light, *New Phytol.*, 207, 159–171, <https://doi.org/10.1111/nph.13334>, 2015.
- Hoppema, M., Fahrbach, E., Schröder, M., Wisotzki, A., and de Baar, H. J.: Winter-summer differences of carbon dioxide and oxygen in the Weddell Sea surface layer, *Mar. Chem.*, 51, 177–192, [https://doi.org/10.1016/0304-4203\(95\)00065-8](https://doi.org/10.1016/0304-4203(95)00065-8), 1995.
- IPCC: Climate Change 2013: The Physical Science Basis. Contribution of Working Group I to the Fifth Assessment Report of the Intergovernmental Panel on Climate Change, Cambridge University Press, Cambridge, UK and New York, NY, USA, <https://doi.org/10.1017/CBO9781107415324>, 2013.
- Jeffrey, S. and Humphrey, G.: New spectrophotometric equations for determining chlorophylls *a*, *b*, *c*<sub>1</sub> and *c*<sub>2</sub> in higher plants, algae and natural phytoplankton, *Biochem. Physiol. Pflanz.*, 167, 191–194, [https://doi.org/10.1016/S0015-3796\(17\)30778-3](https://doi.org/10.1016/S0015-3796(17)30778-3), 1975.
- Jeffrey, S. W. and Wright, S. W.: Qualitative and quantitative HPLC analysis of SCOR reference algal cultures, in: *Phytoplankton Pigments in Oceanography: Guidelines to Modern Methods*, edited by: Jeffrey, S., Mantoura, R., and Wright, S., 343–360, UNESCO, Paris, 1997.
- Kähler, P. and Koeve, W.: Marine dissolved organic matter: Can its C:N ratio explain carbon overconsumption?, *Deep-Sea Res. Part I*, 48, 49–62, [https://doi.org/10.1016/S0967-0637\(00\)00034-0](https://doi.org/10.1016/S0967-0637(00)00034-0), 2001.
- Khatiwala, S., Primeau, F., and Hall, T.: Reconstruction of the history of anthropogenic CO<sub>2</sub> concentrations in the ocean, *Nature*, 462, 346–349, <https://doi.org/10.1038/nature08526>, 2009.
- Kim, J.-M., Lee, K., Shin, K., Kang, J.-H., Lee, H.-W., Kim, M., Jang, P.-G., and Jang, M.-C.: The effect of seawater CO<sub>2</sub> concentration on growth of a natural phytoplankton assemblage in a controlled mesocosm experiment, *Limnol. Oceanogr.*, 51, 1629–1636, <https://doi.org/10.4319/lo.2006.51.4.1629>, 2006.
- King, A., Jenkins, B., Wallace, J., Liu, Y., Wikfors, G., Milke, L., and Meseck, S.: Effects of CO<sub>2</sub> on growth rate, C:N:P, and fatty acid composition of seven marine phytoplankton species, *Mar. Ecol. Prog. Ser.*, 537, 59–69, <https://doi.org/10.3354/meps11458>, 2015.
- Kirchman, D. L.: Measuring Bacterial Biomass Production and Growth Rates from Leucine Incorporation in Natural Aquatic Environments, in: *Methods in Microbiology*, edited by: Paul, J., vol. 30, chap. 12, 227–237, Academic Press, St. Petersburg, FL, [https://doi.org/10.1016/S0580-9517\(01\)30047-8](https://doi.org/10.1016/S0580-9517(01)30047-8), 2001.
- Kirchman, D. L.: *Microbial ecology of the oceans*, Wiley-Blackwell, Hoboken, NJ, 2 edn., 620 pp., 2008.
- Legendre, L., Ackley, S. F., Dieckmann, G. S., Gulliksen, B., Horner, R., Hoshiai, T., Melnikov, I. A., Reeburgh, W. S., Spindler, M., and Sullivan, C. W.: Ecology of sea ice biota – 2. Global significance, *Polar Biol.*, 12, 429–444, <https://doi.org/10.1007/BF00243114>, 1992.
- Lewis, M. and Smith, J.: A small volume, short-incubation-time method for measurement of photosynthesis as a function of incident irradiance, *Mar. Ecol. Prog. Ser.*, 13, 99–102, <https://doi.org/10.3354/meps013099>, 1983.
- Li, F., Beardall, J., Collins, S., and Gao, K.: Decreased photosynthesis and growth with reduced respiration in the model diatom *Phaeodactylum tricornutum* grown under elevated CO<sub>2</sub> over 1800 generations, *Global Change Biol.*, 23, 127–137, <https://doi.org/10.1111/gcb.13501>, 2017a.
- Li, W., Yang, Y., Li, Z., Xu, J., and Gao, K.: Effects of seawater acidification on the growth rates of the diatom *Thalassiosira (Conticribra) weissflogii* under different nutrient, light, and UV radiation regimes, *J. Appl. Phycol.*, 29, 133–142, <https://doi.org/10.1007/s10811-016-0944-y>, 2017b.
- Liu, N., Beardall, J., and Gao, K.: Elevated CO<sub>2</sub> and associated seawater chemistry do not benefit a model diatom grown with increased availability of light, *Aquat. Microb. Ecol.*, 79, 137–147, <https://doi.org/10.3354/ame01820>, 2017.
- Longhurst, A. R.: Role of the marine biosphere in the global carbon cycle, *Limnol. Oceanogr.*, 36, 1507–1526, <https://doi.org/10.4319/lo.1991.36.8.1507>, 1991.
- Lueker, T. J., Dickson, A. G., and Keeling, C. D.: Ocean pCO<sub>2</sub> calculated from dissolved inorganic carbon, alkalinity, and equations for K<sub>1</sub> and K<sub>2</sub>: validation based on laboratory measurements of CO<sub>2</sub> in gas and seawater at equilibrium, *Mar. Chem.*, 70, 105–119, [https://doi.org/10.1016/S0304-4203\(00\)00022-0](https://doi.org/10.1016/S0304-4203(00)00022-0), 2000.
- Mantoura, R. and Repeta, D.: Calibration methods for HPLC, in: *Phytoplankton Pigments in Oceanography: Guidelines to Modern Methods*, edited by: Jeffrey, S., Mantoura, R., and Wright, S., 407–428, UNESCO, Paris, 1997.
- Marie, D., Simon, N., and Vaulot, D.: Phytoplankton cell counting by flow cytometry, in: *Algal Culturing Techniques*, edited by: Anderson, R. A., chap. 17, 253–267, Academic Press, San Diego, CA, USA, <https://doi.org/10.1016/B978-012088426-1/50018-4>, 2005.
- McMinn, A., Müller, M. N., Martin, A., and Ryan, K. G.: The Response of Antarctic Sea Ice Algae to Changes in pH and CO<sub>2</sub>, *PLoS One*, 9, e86984, <https://doi.org/10.1371/journal.pone.0086984>, 2014.
- McNeil, B. I. and Matear, R. J.: Southern Ocean acidification: A tipping point at 450-ppm atmospheric CO<sub>2</sub>, *P. Natl. Acad. Sci.*, 105, 18860–18864, <https://doi.org/10.1073/pnas.0806318105>, 2008.
- Mehrbach, C., Culbertson, C. H., Hawley, J. E., and Pytkowicz, R. M.: Measurement of the Apparent Dissociation Constants of Carbonic Acid in Seawater At Atmospheric Pressure, *Limnol. Oceanogr.*, 18, 897–907, <https://doi.org/10.4319/lo.1973.18.6.0897>, 1973.
- Meinshausen, M., Smith, S. J., Calvin, K., Daniel, J. S., Kainuma, M. L. T., Lamarque, J., Matsumoto, K., Montzka, S. A., Raper, S. C. B., Riahi, K., Thomson, A., Velders, G. J. M., and van Vuuren, D. P. P.: The RCP greenhouse gas concentrations and their extensions from 1765 to 2300, *Clim. Change*, 109, 213–241, <https://doi.org/10.1007/s10584-011-0156-z>, 2011.
- Metzl, N., Tilbrook, B., and Poisson, A.: The annual *f*CO<sub>2</sub> cycle and the air-sea CO<sub>2</sub> flux in the sub-Antarctic Ocean, *Tellus B*, 51, 849–861, <https://doi.org/10.1034/j.1600-0889.1999.t013-00008.x>, 1999.
- Moreau, S., Schloss, I., Mostajir, B., Demers, S., Almandoz, G., Ferrario, M., and Ferreyra, G.: Influence of microbial community composition and metabolism on air-sea ΔpCO<sub>2</sub> variation off the

- western Antarctic Peninsula, *Mar. Ecol. Prog. Ser.*, 446, 45–59, <https://doi.org/10.3354/meps09466>, 2012.
- Nelson, D. M., Smith, W. O. J., Gordon, L. I., and Huber, B. A.: Spring distributions of density, nutrients, and phytoplankton biomass in the ice edge zone of the Weddell-Scotia Sea, *J. Geophys. Res.-Ocean.*, 92, 7181, <https://doi.org/10.1029/JC092iC07p07181>, 1987.
- Orr, J. C., Fabry, V. J., Aumont, O., Bopp, L., Doney, S. C., Feely, R. A., Gnanadesikan, A., Gruber, N., Ishida, A., Joos, F., Key, R. M., Lindsay, K., Maier-Reimer, E., Matear, R., Monfray, P., Mouchet, A., Najjar, R. G., Plattner, G.-K., Rodgers, K. B., Sabine, C. L., Sarmiento, J. L., Schlitzer, R., Slater, R. D., Totterdell, I. J., Weirig, M.-F., Yamanaka, Y., and Yool, A.: Anthropogenic ocean acidification over the twenty-first century and its impact on calcifying organisms, *Nature*, 437, 681–686, <https://doi.org/10.1038/nature04095>, 2005.
- Pasquer, B., Mongin, M., Johnston, N., and Wright, S.: Distribution of particulate organic matter (POM) in the Southern Ocean during BROKE-West (30°E - 80°E), *Deep-Sea Res. Part II*, 57, 779–793, <https://doi.org/10.1016/j.dsr2.2008.12.040>, 2010.
- Paul, C., Matthiessen, B., and Sommer, U.: Warming, but not enhanced CO<sub>2</sub> concentration, quantitatively and qualitatively affects phytoplankton biomass, *Mar. Ecol. Prog. Ser.*, 528, 39–51, <https://doi.org/10.3354/meps11264>, 2015.
- Paulino, A. I., Egge, J. K., and Larsen, A.: Effects of increased atmospheric CO<sub>2</sub> on small and intermediate sized osmotrophs during a nutrient induced phytoplankton bloom, *Biogeosciences*, 5, 739–748, <https://doi.org/10.5194/bg-5-739-2008>, 2008.
- Pearce, I., Davidson, A., Bell, E., and Wright, S.: Seasonal changes in the concentration and metabolic activity of bacteria and viruses at an Antarctic coastal site, *Aquat. Microb. Ecol.*, 47, 11–23, <https://doi.org/10.3354/ame047011>, 2007.
- Pearce, I., Davidson, A. T., Thomson, P. G., Wright, S., and van den Enden, R.: Marine microbial ecology off East Antarctica (30–80° E): Rates of bacterial and phytoplankton growth and grazing by heterotrophic protists, *Deep-Sea Res. Part II*, 57, 849–862, <https://doi.org/10.1016/j.dsr2.2008.04.039>, 2010.
- Perrin, R. A., Lu, P., and Marchant, H. J.: Seasonal variation in marine phytoplankton and ice algae at a shallow Antarctic coastal site, *Hydrobiologia*, 146, 33–46, <https://doi.org/10.1007/BF00007575>, 1987.
- Petrou, K., Kranz, S. A., Trimborn, S., Hassler, C. S., Ameijeiras, S. B., Sackett, O., Ralph, P. J., and Davidson, A. T.: Southern Ocean phytoplankton physiology in a changing climate, *J. Plant Physiol.*, 203, 135–150, <https://doi.org/10.1016/j.jplph.2016.05.004>, 2016.
- Piontek, J., Borchard, C., Sperling, M., Schulz, K. G., Riebesell, U., and Engel, A.: Response of bacterioplankton activity in an Arctic fjord system to elevated pCO<sub>2</sub>: results from a mesocosm perturbation study, *Biogeosciences*, 10, 297–314, <https://doi.org/10.5194/bg-10-297-2013>, 2013.
- Platt, T., Gallegos, C. L., and Harrison, W. G.: Photoinhibition of photosynthesis in natural assemblages of marine phytoplankton, *J. Mar. Res.*, 38, 687–701, 1980.
- Polimene, L., Sailley, S., Clark, D., Mitra, A., and Allen, J. I.: Biological or microbial carbon pump? The role of phytoplankton stoichiometry in ocean carbon sequestration, *J. Plankton Res.*, 39, 180–186, <https://doi.org/10.1093/plankt/fbw091>, 2016.
- R Core Team: R: A Language and Environment for Statistical Computing, R Foundation for Statistical Computing, Vienna, Austria, <https://www.R-project.org/> (last access: 11 December 2017), 2016.
- Raven, J. A.: Physiology of inorganic C acquisition and implications for resource use efficiency by marine phytoplankton: relation to increased CO<sub>2</sub> and temperature, *Plant, Cell Environ.*, 14, 779–794, <https://doi.org/10.1111/j.1365-3040.1991.tb01442.x>, 1991.
- Raven, J. A. and Falkowski, P. G.: Oceanic sinks for atmospheric CO<sub>2</sub>, *Plant, Cell Environ.*, 22, 741–755, <https://doi.org/10.1046/j.1365-3040.1999.00419.x>, 1999.
- Raven, J. A., Caldeira, K., Elderfield, H., Hoegh-Guldberg, O., Liss, P., Riebesell, U., Shepherd, J., Turley, C., and Watson, A.: Ocean acidification due to increasing atmospheric carbon dioxide, *Tech. Rep. June*, The Royal Society, 2005.
- Regaudie-de Gioux, A., Lasternas, S., Agustí, S., Duarte, C. M., and Benitez, N. G.: Comparing marine primary production estimates through different methods and development of conversion equations, *Front. Mar. Sci.*, 1, 1–14, <https://doi.org/10.3389/fmars.2014.00019>, 2014.
- Riebesell, U.: Effects of CO<sub>2</sub> Enrichment on Marine Phytoplankton, *J. Oceanogr.*, 60, 719–729, <https://doi.org/10.1007/s10872-004-5764-z>, 2004.
- Riebesell, U., Schulz, K. G., Bellerby, R. G. J., Botros, M., Fritsche, P., Meyerhöfer, M., Neill, C., Nondal, G., Oschlies, A., Wohlers, J., and Zöllner, E.: Enhanced biological carbon consumption in a high CO<sub>2</sub> ocean, *Nature*, 450, 545–548, <https://doi.org/10.1038/nature06267>, 2007.
- Riebesell, U., Gattuso, J.-P., Thingstad, T. F., and Middelburg, J. J.: Preface “Arctic ocean acidification: pelagic ecosystem and biogeochemical responses during a mesocosm study”, *Biogeosciences*, 10, 5619–5626, <https://doi.org/10.5194/bg-10-5619-2013>, 2013.
- Riley, G. A.: Phytoplankton of the North Central Sargasso Sea, 1950–521, *Limnol. Oceanogr.*, 2, 252–270, <https://doi.org/10.1002/lno.1957.2.3.0252>, 1957.
- Ritchie, R. J.: Consistent sets of spectrophotometric chlorophyll equations for acetone, methanol and ethanol solvents, *Photosynth. Res.*, 89, 27–41, <https://doi.org/10.1007/s11120-006-9065-9>, 2006.
- Roden, N. P., Shadwick, E. H., Tilbrook, B., and Trull, T. W.: Annual cycle of carbonate chemistry and decadal change in coastal Prydz Bay, East Antarctica, *Mar. Chem.*, 155, 135–147, <https://doi.org/10.1016/j.marchem.2013.06.006>, 2013.
- Rost, B., Riebesell, U., Burkhardt, S., and Sültemeyer, D.: Carbon acquisition of bloom-forming marine phytoplankton, *Limnol. Oceanogr.*, 48, 55–67, <https://doi.org/10.4319/lo.2003.48.1.0055>, 2003.
- Sabine, C. L., Feely, R. A., Gruber, N., Key, R. M., Lee, K., Bullister, J. L., Wanninkhof, R., Wong, C. S., Wallace, D. W. R., Tilbrook, B., Millero, F. J., Peng, T.-H., Kozyr, A., Ono, T., and Rios, A. F.: The Oceanic Sink for Anthropogenic CO<sub>2</sub>, *Science*, 305, 367–371, <https://doi.org/10.1126/science.1097403>, 2004.
- Satoh, A., Kurano, N., and Miyachi, S.: Inhibition of photosynthesis by intracellular carbonic anhydrase in microalgae under excess concentrations of CO<sub>2</sub>, *Photosynth. Res.*, 68, 215–224, <https://doi.org/10.1023/A:1012980223847>, 2001.

- Schaum, C. E. and Collins, S.: Plasticity predicts evolution in a marine alga, *P. R. Soc. B Biol. Sci.*, 281, 1793, <https://doi.org/10.1098/rspb.2014.1486>, 2014.
- Schaum, E., Rost, B., Millar, A. J., and Collins, S.: Variation in plastic responses of a globally distributed picoplankton species to ocean acidification, *Nat. Clim. Change*, 3, 298–302, <https://doi.org/10.1038/nclimate1774>, 2012.
- Schreiber, U.: Pulse-Amplitude-Modulation (PAM) Fluorometry and Saturation Pulse Method: An Overview, in: *Chlorophyll a Fluorescence*, edited by: Papageorgiou, G. C. and Govindjee, 279–319, Springer Netherlands, Dordrecht, [https://doi.org/10.1007/978-1-4020-3218-9\\_11](https://doi.org/10.1007/978-1-4020-3218-9_11), 2004.
- Schulz, K. G., Bellerby, R. G. J., Brussaard, C. P. D., Büdenbender, J., Czerny, J., Engel, A., Fischer, M., Koch-Klavnsen, S., Krug, S. A., Lischka, S., Ludwig, A., Meyerhöfer, M., Nondal, G., Silyakova, A., Stühr, A., and Riebesell, U.: Temporal biomass dynamics of an Arctic plankton bloom in response to increasing levels of atmospheric carbon dioxide, *Biogeosciences*, 10, 161–180, <https://doi.org/10.5194/bg-10-161-2013>, 2013.
- Schulz, K. G., Bach, L. T., Bellerby, R. G. J., Bermúdez, R., Büdenbender, J., Boxhammer, T., Czerny, J., Engel, A., Ludwig, A., Meyerhöfer, M., Larsen, A., Paul, A. J., Sswat, M., and Riebesell, U.: Phytoplankton Blooms at Increasing Levels of Atmospheric Carbon Dioxide: Experimental Evidence for Negative Effects on Prymnesiophytes and Positive on Small Picoeukaryotes, *Front. Mar. Sci.*, 4, 1–18, <https://doi.org/10.3389/fmars.2017.00064>, 2017.
- Shi, D., Xu, Y., and Morel, F. M. M.: Effects of the pH/pCO<sub>2</sub> control method on medium chemistry and phytoplankton growth, *Biogeosciences*, 6, 1199–1207, <https://doi.org/10.5194/bg-6-1199-2009>, 2009.
- Shi, Q., Xiahou, W., and Wu, H.: Photosynthetic responses of the marine diatom *Thalassiosira pseudonana* to CO<sub>2</sub>-induced seawater acidification, *Hydrobiologia*, 788, 361–369, <https://doi.org/10.1007/s10750-016-3014-1>, 2017.
- Silsbe, G. M. and Malkin, S. Y.: phytotools: Phytoplankton Production Tools, <https://CRAN.R-project.org/package=phytotools> (last access: 11 December 2017), R package version 1.0, 2015.
- Simon, M. and Azam, F.: Protein content and protein synthesis rates of planktonic marine bacteria, *Mar. Ecol. Prog. Ser.*, 51, 201–213, <https://doi.org/10.3354/meps051201>, 1989.
- Smith, W. O. and Nelson, D. M.: Importance of Ice Edge Phytoplankton Production in the Southern Ocean, *BioScience*, 36, 251–257, <https://doi.org/10.2307/1310215>, 1986.
- Sobrinho, C., Ward, M. L., and Neale, P. J.: Acclimation to elevated carbon dioxide and ultraviolet radiation in the diatom *Thalassiosira pseudonana*: Effects on growth, photosynthesis, and spectral sensitivity of photoinhibition, *Limnol. Oceanogr.*, 53, 494–505, <https://doi.org/10.4319/lo.2008.53.2.0494>, 2008.
- Sommer, U., Paul, C., and Moustaka-Gouni, M.: Warming and Ocean Acidification Effects on Phytoplankton—From Species Shifts to Size Shifts within Species in a Mesocosm Experiment, *PLoS One*, 10, e0125239, <https://doi.org/10.1371/journal.pone.0125239>, 2015.
- Sperling, M., Piontek, J., Gerdt, G., Wichels, A., Schunck, H., Roy, A.-S., La Roche, J., Gilbert, J., Nissimov, J. I., Bittner, L., Romac, S., Riebesell, U., and Engel, A.: Effect of elevated CO<sub>2</sub> on the dynamics of particle-attached and free-living bacterioplankton communities in an Arctic fjord, *Biogeosciences*, 10, 181–191, <https://doi.org/10.5194/bg-10-181-2013>, 2013.
- Spilling, K., Paul, A. J., Virkkala, N., Hastings, T., Lischka, S., Stühr, A., Bermúdez, R., Czerny, J., Boxhammer, T., Schulz, K. G., Ludwig, A., and Riebesell, U.: Ocean acidification decreases plankton respiration: evidence from a mesocosm experiment, *Biogeosciences*, 13, 4707–4719, <https://doi.org/10.5194/bg-13-4707-2016>, 2016.
- Steemann Nielsen, E.: The Use of Radio-active Carbon (C<sup>14</sup>) for Measuring Organic Production in the Sea, *ICES J. Mar. Sci.*, 18, 117–140, <https://doi.org/10.1093/icesjms/18.2.117>, 1952.
- Takahashi, T., Sutherland, S. C., Wanninkhof, R., Sweeney, C., Feely, R. A., Chipman, D. W., Hales, B., Friederich, G., Chavez, F., Sabine, C., Watson, A., Bakker, D. C., Schuster, U., Metzl, N., Yoshikawa-Inoue, H., Ishii, M., Midorikawa, T., Nojiri, Y., Körtzinger, A., Steinhoff, T., Hoppema, M., Olafsson, J., Arnarson, T. S., Tilbrook, B., Johannessen, T., Olsen, A., Bellerby, R., Wong, C., Delille, B., Bates, N., and de Baar, H. J.: Climatological mean and decadal change in surface ocean pCO<sub>2</sub>, and net sea–air CO<sub>2</sub> flux over the global oceans, *Deep-Sea Res. Part II*, 56, 554–577, <https://doi.org/10.1016/j.dsr2.2008.12.009>, 2009.
- Takahashi, T., Sweeney, C., Hales, B., Chipman, D., Newberger, T., Goddard, J., Iannuzzi, R., and Sutherland, S.: The Changing Carbon Cycle in the Southern Ocean, *Oceanography*, 25, 26–37, <https://doi.org/10.5670/oceanog.2012.71>, 2012.
- Tanaka, T., Alliouane, S., Bellerby, R. G. B., Czerny, J., de Kluijver, A., Riebesell, U., Schulz, K. G., Silyakova, A., and Gattuso, J.-P.: Effect of increased pCO<sub>2</sub> on the planktonic metabolic balance during a mesocosm experiment in an Arctic fjord, *Biogeosciences*, 10, 315–325, <https://doi.org/10.5194/bg-10-315-2013>, 2013.
- Taylor, A. R., Brownlee, C., and Wheeler, G. L.: Proton channels in algae: reasons to be excited, *Trends Plant Sci.*, 17, 675–684, <https://doi.org/10.1016/j.tplants.2012.06.009>, 2012.
- Tew, K. S., Kao, Y.-C., Ko, F.-C., Kuo, J., Meng, P.-J., Liu, P.-J., and Glover, D. C.: Effects of elevated CO<sub>2</sub> and temperature on the growth, elemental composition, and cell size of two marine diatoms: potential implications of global climate change, *Hydrobiologia*, 741, 79–87, <https://doi.org/10.1007/s10750-014-1856-y>, 2014.
- Thomson, P., Davidson, A., and Maher, L.: Increasing CO<sub>2</sub> changes community composition of pico- and nano-sized protists and prokaryotes at a coastal Antarctic site, *Mar. Ecol. Prog. Ser.*, 554, 51–69, <https://doi.org/10.3354/meps11803>, 2016.
- Torstensson, A., Hedblom, M., Mattsdotter Björk, M., Chierici, M., and Wulff, A.: Long-term acclimation to elevated pCO<sub>2</sub> alters carbon metabolism and reduces growth in the Antarctic diatom *Nitzschia lecontei*, *P. R. Soc. B*, 282, 20151513, <https://doi.org/10.1098/rspb.2015.1513>, 2015.
- Tortell, P. D. and Morel, F. M. M.: Sources of inorganic carbon for phytoplankton in the eastern Subtropical and Equatorial Pacific Ocean, *Limnol. Oceanogr.*, 47, 1012–1022, <https://doi.org/10.4319/lo.2002.47.4.1012>, 2002.
- Tortell, P. D., Rau, G. H., and Morel, F. M. M.: Inorganic carbon acquisition in coastal Pacific phytoplankton communities, *Limnol. Oceanogr.*, 45, 1485–1500, <https://doi.org/10.4319/lo.2000.45.7.1485>, 2000.
- Tortell, P. D., Payne, C., Gueguen, C., Strzepak, R. F., Boyd, P. W., and Rost, B.: Inorganic carbon uptake by South-

- ern Ocean phytoplankton, *Limnol. Oceanogr.*, 53, 1266–1278, <https://doi.org/10.4319/lo.2008.53.4.1266>, 2008a.
- Tortell, P. D., Payne, C. D., Li, Y., Trimborn, S., Rost, B., Smith, W. O. J., Riesselman, C., Dunbar, R. B., Sedwick, P., and DiTullio, G. R.: CO<sub>2</sub> sensitivity of Southern Ocean phytoplankton, *Geophys. Res. Lett.*, 35, L04605, <https://doi.org/10.1029/2007GL032583>, 2008b.
- Tortell, P. D., Trimborn, S., Li, Y., Rost, B., and Payne, C. D.: Inorganic carbon utilization by Ross Sea phytoplankton across natural and experimental CO<sub>2</sub> gradients, *J. Phycol.*, 46, 433–443, <https://doi.org/10.1111/j.1529-8817.2010.00839.x>, 2010.
- Tortell, P. D., Asher, E. C., Ducklow, H. W., Goldman, J. A. L., Dacey, J. W. H., Grzyski, J. J., Young, J. N., Kranz, S. A., Bernard, K. S., and Morel, F. M. M.: Metabolic balance of coastal Antarctic waters revealed by autonomous pCO<sub>2</sub> and ΔO<sub>2</sub>/Ar measurements, *Geophys. Res. Lett.*, 41, 6803–6810, <https://doi.org/10.1002/2014GL061266>, 2014.
- Trimborn, S., Brenneis, T., Sweet, E., and Rost, B.: Sensitivity of Antarctic phytoplankton species to ocean acidification: Growth, carbon acquisition, and species interaction, *Limnol. Oceanogr.*, 58, 997–1007, <https://doi.org/10.4319/lo.2013.58.3.0997>, 2013.
- Trimborn, S., Thoms, S., Petrou, K., Kranz, S. A., and Rost, B.: Photophysiological responses of Southern Ocean phytoplankton to changes in CO<sub>2</sub> concentrations: Short-term versus acclimation effects, *J. Exp. Mar. Bio. Ecol.*, 451, 44–54, <https://doi.org/10.1016/j.jembe.2013.11.001>, 2014.
- van de Waal, D. B., Verschoor, A. M., Verspagen, J. M., van Donk, E., and Huisman, J.: Climate-driven changes in the ecological stoichiometry of aquatic ecosystems, *Front. Ecol. Environ.*, 8, 145–152, <https://doi.org/10.1890/080178>, 2010.
- Wang, Y., Zhang, R., Zheng, Q., Deng, Y., Van Nostrand, J. D., Zhou, J., and Jiao, N.: Bacterioplankton community resilience to ocean acidification: evidence from microbial network analysis, *ICES J. Mar. Sci. J. du Cons.*, 73, 865–875, <https://doi.org/10.1093/icesjms/fsv187>, 2016.
- Westwood, K., Thomson, P., van den Enden, R., Maher, L., Wright, S., and Davidson, A.: Ocean acidification impacts primary and bacterial production in Antarctic coastal waters during austral summer, *J. Exp. Mar. Bio. Ecol.*, 498, 46–60, <https://doi.org/10.1016/j.jembe.2017.11.003>, 2018.
- Westwood, K. J., Brian Griffiths, F., Meiners, K. M., and Williams, G. D.: Primary productivity off the Antarctic coast from 30°–80° E; BROKE-West survey, 2006, *Deep-Sea Res. Part II*, 57, 794–814, <https://doi.org/10.1016/j.dsr2.2008.08.020>, 2010.
- Wright, S. W., van den Enden, R. L., Pearce, I., Davidson, A. T., Scott, F. J., and Westwood, K. J.: Phytoplankton community structure and stocks in the Southern Ocean (30–80° E) determined by CHEMTAX analysis of HPLC pigment signatures, *Deep-Sea Res. Part II*, 57, 758–778, <https://doi.org/10.1016/j.dsr2.2009.06.015>, 2010.
- Wu, Y., Gao, K., and Riebesell, U.: CO<sub>2</sub>-induced seawater acidification affects physiological performance of the marine diatom *Phaeodactylum tricornutum*, *Biogeosciences*, 7, 2915–2923, <https://doi.org/10.5194/bg-7-2915-2010>, 2010.
- Young, J., Kranz, S., Goldman, J., Tortell, P., and Morel, F.: Antarctic phytoplankton down-regulate their carbon-concentrating mechanisms under high CO<sub>2</sub> with no change in growth rates, *Mar. Ecol. Prog. Ser.*, 532, 13–28, <https://doi.org/10.3354/meps11336>, 2015.
- Zheng, Y., Giordano, M., and Gao, K.: Photochemical responses of the diatom *Skeletonema costatum* grown under elevated CO<sub>2</sub> concentrations to short-term changes in pH, *Aquat. Biol.*, 23, 109–118, <https://doi.org/10.3354/ab00619>, 2015.